LA-UR- 97-3581

Approved for public release; distribution is unlimited.

Title: Mitigation of Atmospheric Carbon Emissions Through Increased Energy Efficiency Versus Increased Non-Carbon Energy Sources: A Trade Study Using a Simplified "Market-Free" Exogenously Driven Model

Author(s): R. A. Krakowski

Submitted to: General Distribution

Los Alamos
NATIONAL LABORATORY

DISCLAIMER

DRAFT

MITIGATION OF ATMOSPHERIC CARBON EMISSIONS THROUGH INCREASED ENERGY EFFICIENCY *VERSUS* INCREASED NON-CARBON ENERGY SOURCES: A TRADE STUDY USING A SIMPLIFIED "MARKET-FREE" EXOGENOUSLY DRIVEN MODEL

R.A. Krakowski

Los Alamos National Laboratory
Los Alamos, New Mexico 87545
August 24, 1997

ABSTRACT

A simplified model of global, long-term energy use is described and used to make a "top-level" comparison of two generic approaches for mitigating atmospheric carbon emissions: a) those based on increased energy efficiency; and b) those based on increased use of reduced- or non-carbon fuels. As approximate as is the model, first-order estimates of and trade offs between increasing non-carbon generation capacities (*e.g.,* supply-side solutions) *versus* energy-use efficiency (*e.g.,* demand-side solutions) to stem atmospheric carbon accumulations can be useful in guiding more elaborate models. At the level of this analysis, both the costs of abatement and the costs of damage can be large, with the formation of benefit-to-cost ratios as a means of assessment being limited by uncertainties associated with relating given climatic responses to greenhouse warming to aggregate damage cost, as well as uncertainties associated with procedures used for multi-generation discounting of both abatement and damage costs. In view of uncertainties associated with both supply-side and demand-side approaches, as well as the estimation of greenhouse-warming responses *per se*, a combination of solutions seems prudent. Key findings are: a) the relative insensitivity of the benefit-to-cost ratio adopted in this study to supply-side *versus* demand-side approaches to abating atmospheric carbon-dioxide emissions; b) the extreme sensitivity of damage costs, abatement costs, and the related benefit-to-cost ratios to the combination of discounting procedure and the (time) concavity of the function used to relate global temperature rise to damage costs; and c) no matter the discounting procedure and/or functional relationship between average temperature rise and a damage cost, a goal of increased *per-capita* gross world product at minimum damage suggests action now rather than delay. These finds, however, must be tempered by obvious limitations of the fully driven nature of the simplified, "market-free" model used; both magnitude (and possibly even the sign) and regionalization of the damage related to greenhouse warming and the degree to which "no regrets" economics are embedded in the estimates of abatement cost represent key uncertainties.

CONTENTS

I. INTRODUCTION

A. Background

Models used to understand long-term energy/economic/environmental (E^3) impacts of specific policies are broadly divided into two classes: "top down" and "bottom up" .[1,2] Top-down models describe energy-economy interactions in a macroeconomic framework.[3-8] The most important exogenous input to top-down models include:[2] a) GNP growth; b) rate of non-price-induced improvements (decreases) in energy intensity; c) elasticities of price-induced substitution between factors of production (*e.g.,* labor, materials, capital, energy); d) key performance metrics of future electricity generation technologies (*e.g.,* availabilities, efficiencies, capital and operating costs); e) cost of electric and non-electric "backstop" technologies (*e.g.,* energy supplies available in essentially unlimited quantity, but a very high costs). Historical market behavior strongly guide the predictive *modus operadi* of top-down models. This dependence on past performance can limit the scope of assessments of technical and institutional innovations and related impacts on costs and productivity, particularly as related to the abatement of greenhouse gases (GHGs). The impacts of progress on both demand and supply sides of the E^3 equation can be missed in these highly aggregated top-down models. General ease of application to examination E^3 interactions/issues on a global (multi-regional) scale using highly developed macroeconomic theories, albeit of limited time horizon, are strong merits of the top-down modeling approach. Generally,[4] top-down modelers conclude that most approaches to mitigating greenhouse warming have a negative impact on the global economy, and a "wait-and-see" position driven by the comforts of discounting future costs (and generations) more often than not emerge from these kinds of studies.

A disaggregated approach to understanding these E^3 issues is taken by analysts who use the bottom-up approach to examine a closely coupled energy supply and demand systems.[9-11] Either directly or indirectly, the solution-oriented bottom-up models address the following constraints that drive predictions of high CO_2 mitigation costs when viewed from the top-down perspective:[1,2]

- high level of aggregations results in a loss of physical reality;
- tendency to project selective past energy-economy relationships into the future;
- rigidity of energy-economy interactions over the far time horizons necessarily considered in dealing with greenhouse warming;
- limited technical progress in either increasing energy end-use efficiency or enlarging renewable energy supplies, as well as impacts of technological innovation of market behavior and market structure;
- difficulty of modeling the importance of irreversibilities arising from technological innovation and infrastructural investments, leading to (non-optimal) bifurcations in technological developments;
- insufficient boldness in pursuing cost-effective efficiency increases, including dealing with institutional (structural) barriers to implementation;
- insufficient credit given to (often secondary or tertiary) external benefits associated with bottom-up approaches (*e.g.*, health and ecological fallout from reduced air pollution, enhanced energy security);
- omission of positive economic impacts related to recycled, revenue-neutral (at least) carbon taxes and emission-permit exchanges;
- uncertainties, inertia, and (relative) rates (of atmospheric change) enter strongly into E^3 policy making, in addition to simply trading costs and benefits to determine optimal paths.

Rather than macroeconomic relationships, bottom-up models use quantitative data to track past and future energy-technology stocks, thereby accounting for inventory retirement, replacement, and the opportunities to implement improvements and innovations. By following the costs of individual technologies, the bottom-up models allow the assessment of cost-effective potentials for installing energy-efficient technologies at both demand and supply sides of the E^3 equation, although the orientation is generally directed to the demand for energy services. The largest problem with the bottom-up models[2] is an inability to projected costs on a global scale; these are regional/country models that would require extensive country-specific analyses before being "added" together to address the global

problem of greenhouse warm, as driven by local sources and impacts. An equally large methodological problem is that market clearing (*i.e.*, supply = demand) cannot be assured using the bottom-up approach. These shortcomings are major when applying these regional, non-market models to describe the global, long-term problem of greenhouse warming. Generally, projections of economic impact generated by the bottom-up models are nil or strongly positive,[9] these solution-oriented approaches project net long-term benefits for the technology and implementation advances adopted, irrespective of what market forces may suggest.

Combinations of top-down and bottom-up approaches have been used to addresses the limitations of both modeling approaches[13,14] and the greenhouse-warming "cost gap"[2] that has developed between projections derived from respective studies. In spite of the somewhat harsh criticism of top-down approaches,[2] many of the concerns listed above are being address by these combined approaches. Furthermore, some of the simpler and more transparent of the top-down models deal in part with these concerns.[15]

B. Motivation

One motivation for the present analysis is the Ref.-16 demand-side (increased efficiency) *versus* supply-side (increase nuclear energy) comparison. The principal findings of that study are:

- "Even a massive worldwide nuclear power program sustained over a period of several decades could not 'solve' the greenhouse problem. Even if it could, the Third World cannot support a major expansion of nuclear power on the scale that would be required in an attempted nuclear solution to greenhouse warming.

- The key to ameliorating future climatic warming caused by the combustion of fossil fuels is to improve the efficiency of energy usage.

- Improving electrical efficiency in nearly seven times more cost effective than nuclear power for abating CO_2 emissions, in the USA."

By requiring nuclear to replace all global coal consumed in the generation of electricity by the year 2050, the first conclusion is a transparent set-up, from which emerges the absurd requirement of a "...29-fold increase in nuclear capacity, requiring that nuclear power plants be built at the average rate of one new 1,000 MW plant every 1.61 days for the next 37 years." With respect to the second finding, the level of improved energy-usage efficiency required to ameliorate future climatic warming caused by the combustion of fossil fuels requires a 41.2% reduction in coal-generated electricity (27,600 TWeh $\rightarrow$ 16,240 TWeh) by the year 2025. Furthermore, the cost of the increased efficiency required to displace this coal-generated electrical consumption amounts to 20 mills/kWeh in 1995, which is assumed to increase linearly to 40 mills/kWeh in 2025. Finally, in using these cost-of-efficiency assumptions to generate the third finding listed above, the Ref.-16 study deflates the availability of nuclear power to 65%, while applying an inflated fixed charge rate of 0.20 1/yr to an equally inflated capital cost of 3.0 $/We to give a cost of electricity of 135.4 mills/kWeh; the factor of seven given in the third finding is simply the ratio 135.4/20. = 6.77, which actually applies only to the year 1995 for the assumptions made. By correcting for the use of the lower (1995) cost of efficiency and a cost of electricity for nuclear energy that is too large by a factor of ~3, this factor of seven can easily become a factor of unity. Additionally, in computing the cost of displacing atmospheric carbon through the use of nuclear power, the difference between the cost of electricity for the latter and the cost of electricity for the coal-fired plants that have been replaced should be used. In this case, the claimed factor of seven in cost between demand-side energy efficiency and supply-side nuclear energy could easily be reversed from that cited in the third finding listed above.

The use of nuclear (electric) power is but one approach to non-carbon (NC) energy generation, which includes sustainable biomass sources. To address the increased efficiency [more specifically, decreased energy intensity, EI(MJ/$) = (primary energy, PE)/(gross world production, GWP)] *versus* NC energy generation approaches to GHG mitigation, a simplified cost-based parametric comparison between NC (supply-side) and EI (demand-side) is made. At the risk of over simplifying the problem, a "market-free", exogenously driven modeling framework is adopted to steer around the complexities of either the top-down or the bottom-up modeling approaches. Ultimately, one or the other (or both) of the latter approaches must be used, however.

II. APPROACH

Whether generated by top-down or bottom-up models, policy recommendations for dealing with the potential damage related to greenhouse warming can be classified as "wait-and-see", adaptive, or mitigative. As suggested above, the former is usually associated with top-down analyses, and the latter generally issues from bottom-up analyses. The mitigative response can be further subdivided into two classes: a) use of fuels that reduce the emissions of greenhouse gases (GHGs); and b) use of less fuel per unit of user (*per capita*) or product (gross national or world economic product, GNP or GWP, respectively). Both mitigative approaches, or combinations thereof, have technological, implementation, and economic constraints: a) the (energy) supply-side approach represented by increased use of reduced- or non-carbon (NC) fuels has both technological and economic risk, as well as being subject to well-known technology diffusion constraints; and b) approaches that focus on the energy demand side through increasing energy efficiency must deal with the diffuseness and inter-connectivity of routes for effective implementation. Additionally, supply-side and demand-side approaches have direct and indirect costs that are not well understood, particularly for demand-side approaches.

A simplified model of global, long-term energy usage is developed to make a "top-level" comparison between schemes for mitigating atmospheric carbon emissions that are base on increased energy efficiency *versus* increased use of NC fuels. Increased energy efficiency is interpreted in terms of reductions in the ratio of annual primary energy use, PE(EJ/yr), to gross world product, GWP(T$), or the primary energy intensity, EI(MJ/$) = PE/GWP. Non-carbon energy sources apply primarily to electricity generation and includes nuclear, hydroelectric, solar, and carbon-conserving biomass sources. Presently, nuclear and hydroelectric are the main NC energy sources, albeit, both contribute minorly to the atmospheric greenhouse-gas inventories during installation.

The goal of this analysis is to assess the relative CO_2 mitigation effectiveness of EI *versus* NC approaches. The approach used specifies exogenous drivers for improvements in the *per-capita* GWP, GPC($/*capita*), and improvement (*e.g.*, decrease) in global energy intensity, EI(MJ/$). By coupling the growth in global population, POP, to the *per-capita* GWP, the rates of GWP and PE growth result. In addition to driving exogenously GPC and EI, the fraction of PE that is electrical energy, f_{EE}, and the fraction of electrical energy

EE (expressed on a thermal-equivalent basis) that is supplied by NC sources, f_{NC}, are also driven exogenously as a function of time. Feedback between GWP and PE and/or EE utilization, *vis à vis* the forced EI dependencies or the use of more costly NC technologies, is not included in this model, which is devoid of these kinds of economic and market considerations. As approximate as is this approach, first order estimates and trade offs between increased NC generation (supply side) *versus* increased energy-use efficiency (demand side) capacities, as related to atmospheric carbon emission rates, R(GtonneC/yr), and accumulations, W(Gtonne), can provide guidance to more elaborate models[15,17] as well as assessing other similar assessments.[16]

The goal of the present analysis does not include amplification or rectification of these kinds of discrepancies, but instead is to present a broader comparison of these two generic approaches to mitigating atmospheric carbon emissions and accumulations. As such, the supply-side approach is described in terms of non-carbon (NC) electric generation schemes, which include nuclear energy. Furthermore, to broaden the scope of supply-side possibilities, the impacts of demand-side measures to mitigating greenhouse warming are expressed in terms of reductions in primary energy intensity, which in principle includes increased efficiencies for both electric and non-electric energy usage. Lastly, since an overarching motivation for optimal use of energy is the increase in "human welfare" that can be experienced in an "acceptable" world environment, *per-capita* gross world product is used as a forcing function that describes desirable goals of improved human economic welfare and the impact these goals have on the emissions and accumulations of greenhouse-warming gases; the limitations of GPC as a human-welfare metric is elaborated in the summary (Sec. V.).

III. MODEL

The driven global energy-climate-economics model is comprised of three parts: a) an aggregated global energy model; and b) a climate-response model; and c) and economics-costing model. In the spirit of this analysis, the energy model is driven by specified forcing functions, does no optimization of energy-growth or GHG-emission routes, and is used only to generate scenarios. The climate-response model adapts an empirical fit[18] to the results from coupled global climate models (CGCMs) that relates CO_2 emission rates to GHG accumulations and average global temperature increases that ensue. The long-term economic impacts of a given (driven) scenario is evaluate using a climate-economics model

adapted in modified (and parametric) form from the literature.[18-20] The following subsections describe each model component (Energy, Climate, Economics).

A. Energy Model

The global energy intensity, EI(MJ/$), and *per-capita* GWP, GPC($/*capita*), are driven exogenously, according to the following expressions:

$$EI(MJ/\$) = (EI_o - EI_f)\, e^{-t/T_{EI}} + EI_f \tag{1}$$

$$GPC(\$/capita) = (GPC_o - GPC_f)\, e^{-t/T_{GPC}} + GPC_f \ , \tag{2}$$

where the initial and final values used are listed in Table I, as are the respective time constants, T_{EI}(yr) and T_{GPC}(yr). With the initial rates of changes ε_{Jo} defined as $(1 - J_f/J_o)/T_J$ (J = EI,GPC), it follows that for these forcing functions the respective normalized (logarithmic) rates are given by

$$\varepsilon_{EI}(1/yr) = \frac{\varepsilon_{EIo}}{(\varepsilon_{EIo}\ T_{EI} + 1)e^{t/T_{EI}} - \varepsilon_{EIo}\ T_{EI}} \tag{3}$$

$$\varepsilon_{GPC}(1/yr) = \frac{\varepsilon_{GPCo}}{(\varepsilon_{GPCo}\ T_{GPC} + 1)e^{t/T_{GPC}} - \varepsilon_{GPCo}\ T_{GPC}} \ . \tag{4}$$

It is noted that ε_{EI} is the same as the "autononous energy efficiency improvement" or AEEI used in Ref.-8, which is also an exogenous input to that model; for BASE1/BASE2 conditions (Table III, T_{EI} = 60 yr, EI_f/EI_o = 2/3), ε_{EI_o} = 0.0056 1/yr and exponentially approaches zero with a time constant of T_{EI}. More detailed econometric models assume AEEI = 0 and allow the model exogenously to determine the relationship between GDP and energy use; these topics are discussed further in Sec. V.

Similar expressions as Eqs. (1) - (4) are that drive the time dependencies of the fraction of total primary energy (PE) demand provided by electricity (EE), f_{EE} = EE/PE, and the fraction of EE that is provided by non-carbon sources, $f_{NC} = EE_{NC}/EE$. The corresponding initial, final, and time-constant values are also listed on Table I. If the carbon emission

coefficient, α(MtonneC/EJ), is similarly specified as a function of time, the rate of global emission of atmospheric carbon is given by

$$R(\text{Mtonne/yr}) = \alpha \; PE \; (1 - f_{EE} \; f_{NC}) \; , \tag{5}$$

where the constants used to describe $\alpha(t)$ are also listed in Table I. The use of a time-dependent carbon emission coefficient reflects the future use of reduced-carbon fossil fuels, although cost and market forces associated with decreased α values are not taken into account by this "market-free" model.

With ε_{EI} and ε_{GPC} specified as a function of time, the rate of growth of global primary energy, $\varepsilon_{PE} = d\mathit{ln}PE/dt$, is determined by

$$\varepsilon_{PE}(1/\text{yr}) = \varepsilon_{EI} + \varepsilon_{GPC} + \varepsilon_{POP} \; , \tag{6}$$

where $\varepsilon_{POP} = d\mathit{ln}POP/dt$ is the population growth rate. Given initial and asymptotic values of global population growth, ε_{POPo} and ε_{POPf}, respectively, and coupling ε_{POP} to GPC assumed as follows:

$$\varepsilon_{POP}(1/\text{yr}) = (\varepsilon_{POPo} - \varepsilon_{POPf}) \frac{GPC_f - GPC}{GPC_f - GPC_o} + \varepsilon_{POPf} \; , \tag{7}$$

these expressions for ε_{PE} and ε_{POP} can be integrated to obtain the time evolution of annual primary energy demand and population, PE and POP, respectively; initial values, PE_o(EJ) and POP_o(B), are listed in Table I. Equation (7) is an *ad hoc* attempt to relate diminished population growth to improved human welfare, as measured in a highly aggregated (and possibly inaccurate/misleading) form (Sec. V.).

Either increased energy-use efficiency (*e.g.*, decreased EI) or replacement of carbon-burning energy sources with NC energy generation displace atmospheric carbon emission. For a given fraction f_{EE} f_{NC}, the rate of atmospheric carbon emission given by Eq. (5)

represents an approximate emissions reduction by a factor EI/EI_o relative to a reference less-efficient situation, which is taken here to occur at time t = 0 (~1995). This assumption neglects any feedback of reduced energy consumption on GWP. Hence, the reduction in atmospheric carbon emission, ΔR, relative to R (*e.g.*, the rate of carbon emission without efficiency improvements would be $R + \Delta R$) is given by

$$\left[\frac{\Delta R}{R}\right]_{EI} = \frac{EI_o}{EI} - 1 \; . \tag{8}$$

Similarly, for the same energy intensity, the value of R given by Eqn. (6) would be increased by $\Delta R = \alpha f_{EE} \, f_{NC} \, PE$ if NC energy sources where replaced by the carbon-burning energy sources that exist at time t. The relative reduction of atmospheric carbon emission achieved through the use of NC sources is given by

$$\left[\frac{\Delta R}{R}\right]_{NC} = \frac{f_{EE} \; f_{NC}}{1 - f_{EE} \; f_{NC}} \; . \tag{9}$$

The reductions $(\Delta R/R)_{EI,NC}$ are assumed to be accompanied by an increased cost of energy non-generation/generation. Some would argue[9] that these differencential costs could be negative, particularly for demand-side (EI) approaches. Generally, a cost is assumed to be associated with those technologies implemented along the primary → secondary → end-use energy chain to accomplish the generation of the same GWP with reduced PE. Similarly, the NC generation technologies may have a incremental generation cost relative to the carbon-burning technologies being displaced. These costs of increased energy efficiency (*e.g.*, decreased EI) or non-carbon energy generation (NC) are expressed in the form of an incremental cost of electricity, ΔCOE(mill/kWeh). With η_{TH} representing a nominal thermal-to-electric conversion efficiency, the following expression gives the cost of atmospheric carbon reduction using either the EI or the NC approach:

$$UC_{EI,NC}(\$/GJ) = \eta_{TH} \; \Delta COE_{EI,NC} / 3.6 \; . \tag{10}$$

The unit costs $UC_{EI,NC}$ are used to estimate to total cost of CO_2 abatement *vis à vis* EI and NC routes.

The climatic and economic impacts of GHG emissions are expressed in terms that are relative to the starting conditions listed in Table I: a "business-as-usual" (BAU) case is defined for the EI and f_{NC} parameters held unchanged from the t = 0 values, EI_o and f_{NCo}, as is listed in Table I. Hence, the cost of CO_2 abatement at time t *via* the reduced-EI route is determined by applying the unit (differential) cost, UC_{EI}(B$/EJ), to the following reduction in PE that results from decreased energy intensity:

$$\frac{\Delta PE}{PE} = \left(\frac{EI_o}{EI} - 1\right)(1 - f_{EE}\ f_{NC}) \ . \tag{11}$$

The energy ΔPE(EJ/yr) is displaced from the source of atmospheric carbon emission as a result of improved energy efficiency at time t relative to the BAU case. The annual charge for this reduced carbon emission is approximated by AC_{EI}(B$/yr) = UC_{EI} ΔPE.

Likewise, relative to the BAU case, the use of NC energy generation is increased by $\Delta EE_{NC} = EE_{NC} - EE_{NCo}$, according to the following expression:

$$\frac{\Delta EE_{NC}}{PE} = f_{EE}\ f_{NC} - \frac{PE_o}{PE}\ f_{EEo}\ f_{NCo} \ . \tag{12}$$

The annual charge for the reduced carbon emission associated with the increased (relative to the BAU case) use of NC energy generation is approximated by AC_{NC}(B$/yr) = UC_{NC} ΔEE_{NC}. The unit cost associated with atmospheric CO_2 abatement by both NC and EI routes is given by

$$UC_A(B\$/Gtonne) = \frac{AC_{EI}\ UC_{EI} + AC_{NC}\ UC_{NC}}{(\alpha/1000)\ (\Delta PE + \Delta EE_{NC})} \ . \tag{13}$$

This expression can be evaluated for the t = 0 parameters in Table I under the assumption that the cost of efficiency improvement adds[16] ΔCOE_{EI} ~ 20 mill/kWeh to the cost of

energy service provided (albeit, the actual savings is 2-3 times this value because of displaced generation capacity, not to mention important secondary and tertiary benefits claimed for displaced capacity[9]), whereas ΔCOE_{NC} ~ 10 mill/kWeh approximates the difference in generation costs for the NC systems compared to the carbon-burning technology that is replaced. An alternative approach equates the unit abatement cost, UC_A, to the marginal damage cost of CO_2 emission, UC_D(B$/GtonneC), which is the total damage over all time $t' > t$ for a unit emission of CO_2 at time t. An estimate of UC_D, however, requires a model that couples long-term climate changes and damages costs to projected CO_2 emission rates. The Linear Integral-Response Climate Model (LIRCM) described in Ref. 18 and the following section is used .

B. Climate-Response Model

The linear integral-response climate model reported in Ref. 18 is combined with the general procedure for estimating "shadow" prices or marginal costs associated with atmospheric carbon emissions and, along with the specific NC *versus* EI mitigation model described above, constitutes the climate-economics model used herein. Although the detailed long-term representation of the climate, as described by coupled global circulation models (CGCMs),[21-23] is a highly nonlinear problem, the use of a linearized integral-response function to describe atmospheric CO_2 accumulations, W(Gtonne), resulting from anthropogenic sources and average global surface temperature increases, $\Delta T(K)$, is justified by resulting radiation forcings that are only a few percent of the average solar heat flux (340 W/m^2). Nonlinearities driven by concentration- and temperature-dependent CO_2 ocean solubilities for temperature increases of only a few degrees should not come into play. Applications of this model under conditions where temperature increases exceed ΔT ~3K are questioned,[18] however. The limits and advantages of formulating a description of climatic responses in terms of linearized response integrals, instead of (traditional) differential equations, are elaborated in Ref. 18.

Given the impulse response $R_W(t - t')$ for the inventory W(GtonneC) of CO_2 at time t resulting from a unit δ-function emission pulse at time $t' < t$, in the linear approximation it follows that atmospheric CO_2 accumulations are given by

$$W(t) = \int_{t_o}^{t} R_W(t - t')\, e(t')\, dt' \ , \tag{14}$$

where the emission rate is e(GtonneC/yr), $e(t < t_o) = 0$, and $W(t < t_o) = W_o$. Following Ref. 18, the industrial period is assumed to start at $t_o = 1800$, at which point $W_o = 594$ GtonneC (289 vppm, given 2.13 GtonneC/vppm); at present, W(1995) = 760 Gtonne (358 vppm).[18]

Similarly, given the global (surface) temperature impulse response function, $R_T^*(t - t')$, which represents the change in global mean temperature at time t produced by a unit δ-function change in W(t'), the induced change in global mean temperature is given by

$$T(t) = \int_{t_o}^{t} R_T^*(t - t')\, (dW/dt')\, dt' \ . \tag{15}$$

Combination of the carbon-cycle and global temperature response models[18] leads to the following expression that relates the response of the climate temperature increase to the emission rate:

$$\Delta T(t) = \int_{t_o}^{t} R_T(t - t')\, e(t')\, dt' \ , \tag{16}$$

where,

$$R(t) = R_T^*(t) + \int_{o}^{t} R_T^*(t - t')\, (dR_W/dt')\, dt' \ , \tag{17}$$

and $\Delta T(t_o) = (d\Delta T/dt)_{t_o} = R_T(t_o) = 0$. The function $R_T(t - t')$ is the net temperature impulse-response function, or the global warming response,[18] and represents the temperature increase at time t resulting from a unit δ-function atmospheric input of CO_2 at $t = t'$. The global warming response function allows for the thermal inertia of the ocean-

atmosphere climate system as well as the slow CO_2 decrease that results from transfers from the atmosphere to other components of the earth carbon cycle. Not included, however, are very long time-constant processes related to carbon sequestering through chemical reactions occurring at the ocean floor.

The integral response functions R_W and R_T^* have been determined from the response of three-dimensional models of the global carbon cycle[23,24] and the coupled ocean-atmosphere climate system,[22] with the resulting responses being closely fitted by the following exponential sums:

$$R_W(t) = A_o^W + \sum_j A_j^W \, e^{-t/t_j^W} \tag{18}$$

$$R_T^*(t) = W_o^{-1} \sum_j A_j^T \, (1 - e^{-t/t_j^T}) \, . \tag{19}$$

The empirically fitted amplitudes and time constants, A_j^i and t_j^i ($i = W,T$), are listed[18] in Table II for the CO_2 response model reported in Ref. 23. Reference 18 gives a range of empirical fits to other models, as well as graphical and textual comparisons and evaluations. Using these two empirical fits and the Eq. (17) definition, the following expression for the global warming response results:

$$W_o \, R_T(t) = \sum_j A_j^T \, (1 - e^{-t/t_j^T}) -$$

$$\left(\sum_j A_j^T \right) \sum_j A_j^W \, (1 - e^{-t/t_j^W}) -$$

$$\sum_{j,j'} \frac{A_j^T \, A_{j'}^W}{1 - t_{j'}^W / t_j^T} \, (e^{-t/t_j^T} - e^{-t/t_{j'}^W}) \, . \tag{20}$$

Following Ref. 18, the emission rate e(t) over the period t_o = 1880 to the present (t_1 = 1995) is described by the following exponential function:

$$\frac{e(t)}{e(t_1)} = \frac{e^{(t - t_o)/\tau_{CO_2}} - 1}{e^{(t_1 - t_o)/\tau_{CO_2}} - 1} , \qquad (21)$$

where τ_{CO_2} is specified to assure continuity of slopes at $t = t_1$ [*e.g.*, if $\varepsilon_R = d\ell nR/dt$, τ_{CO_2} is solution to $\varepsilon_R \tau_{CO_2}(1 - \tau_{CO_2})(1 - e^{(t_1 - t_o)/\tau_{CO_2}}) = 1$, and $R(0) = e(t_1)$]. Since ΔT computed using this procedure is referenced to the dawn of the industrial revolution (t_o = 1800), and the match in both magnitude and slope is made through the emission rate at t_1 = 1995, studies that vary parameters the influence $R(t_1)$ will give some differences in $\Delta T(t_1)$; these minor differences are an artifact of this model, and appear in some of the graphical results.

C. Economic/Cost Model

The global temperature rise, $\Delta T(t)$, is related to a damage cost through a parameterized damage cost function.[5,18,20] Combining the specificity of the Ref.-23 use of this cost function and the generality of the Ref.-18 usage leads to the following expression:

$$H(B\$/yr) = \left\{k_T (\Delta T/T_{REF})^{\nu_T} + k_{DT}[(d\Delta T/dt)/(d\Delta T/dt)_{REF}]^{\nu_{DT}}\right\} GWP . \qquad (22)$$

This formalism suggests that climate (economic) damage is incurred both through a temperature increase, $\Delta T(t)$, and through the rate of temperature rise, $d\Delta T/dt$. The latter damage[18] reflects added costs associated with adjustments of ecological and human activities that cannot track an overly rapid increase in temperature. This damage cost function expresses cost in terms of the respective fractions, k_T and k_{DT}, of GWP. With interest only in relative changes, Ref. 18 equates these fractions and GWP to unity. The powers ν_T and ν_{DT} are 2 in Ref. 18, whereas other studies[5,20] assume linear dependencies. In the present study, k_{DT} = 0.0 and ν_T is parametrically varied over the

range $\nu_T \equiv \nu = 0.5$(downward concavity) $\rightarrow$ 2.0(upward concavity). As will be shown (Sec. IV.A.), the impact of the concavity of this H-T relationship on the present value of total damage cost, PC_D, depending on degree of discounting, can be important; for the same reference values k_{REF} and T_{REF}, $\nu < 1$ incurs greater earlier cost and present-value weighting than for a $\nu > 1$ scaling, in spite of lower longer-term costs for the latter.

The derivative $(dH/dW)_t$ times the amount of CO_2 remaining in the atmosphere at time t after a unit emission at time $t' < t$ [*e.g.*, $R_W(t-t')$] defines a marginal cost function, $h(t,t')$, as follows:

$$h(t,t')\ (B\$/GtonneC/yr) = \nu_T\ [H(t)/T]\ )d\Delta T/dt)\ R(t - t') \quad . \tag{23}$$

Integration of the marginal cost function over time t', after discounting at a rate r(1/yr), gives the following marginal (unit) damage cost of emitting a unit of CO_2 at time t:

$$UC_D(B\$/Gtonne) = \int_t^{\infty} \frac{h(t,t')}{(1 + r)^{t'-t}}\ dt' \quad . \tag{24}$$

The choice of discount rate is crucial to any benefit-to-cost analysis, because of the long-term nature of the global-warming problem. Taking the view that the cost of climate change will be incurred by mankind without preference to specific generations, and that the welfare of future generations should be given equal weight, a zero rate of time preference should be used.[20] This view on inter-generational equity also characterizes assessments of future risks associated with nuclear waste disposal. Discounting at a rate that reflects the future growth of *per-capita* income (*e.g.*, ε_{GPC}) is justified, however. The following expression for r (Ramsey's rule[5,20]) captures both possibilities:

$$r(1/yr) = \gamma\ \varepsilon_{GPC} + r_o \quad , \tag{25}$$

where γ is the negative of the elasticity of marginal utility of consumption (EMUC),[5,20] $\varepsilon_{GPC}(t)$ is the *per-capita* GWP growth rate, and r_o is the rate of pure time preference. For

all computations reported herein, $r_o = 0.0$, and ε_{GPC} is given by the driver function in Eq. (4).

Equating the abatement unit cost, UC_A(B$/GtonneC), to the unit cost of climate damage, UC_D(B$/GtonneC), gives the following "budget equation" or indifference relationship between the unit cost for CO_2 abatement through increased energy efficiency, UC_{EI}(B$/EJ), *versus* the increased use NC energy generation, UC_{NC}(B$/EJ):

$$UC_{EI} = m\ UC_{NC} + b \ , \tag{26A}$$

where the slope m and intercept b of this (time-dependent) indifference relationship are given by

$$m(t) = \frac{f_{EE}\ f_{NC} - f_{EEo}\ f_{NCo}\ (PE_o / PE)}{(EI_c / EI - 1)\ (1 - f_{EE} f_{NC})} \tag{26B}$$

$$b(\gamma,\nu,t) = (\alpha / 1.000)\ UC_D\ (1 + m) \ . \tag{26C}$$

The nature of this driven model gives m(t) as an exogenous variable; the parameter $b(\gamma,\nu,t)$ is also exogenously determined, as well as being dependent on both the damage cost function and the rule used for discounting [Eq. (25)].

Since neither political, social, nor market forces are represented in this model, the preference for choices that balance EI *versus* NC approaches to GHG mitigation is made through the somewhat *ad hoc* logit-based expression[15] for the cost-based share adopted for either. Specifically, the share of EI and NC abatement schemes, S_j(j= EI,NC) is assumed to be described by

$$S_j = \frac{b_j / (UC_j)^{r_j}}{\sum_j b_j / (UC_j)^{r_j}} \ , \tag{27}$$

where b_j are (market- or policy-determined) weights and $r_j > 0$ are price elasticities. With $\beta = b_{NC}/b_{EI}$ and $\rho = r_{EI}/r_{NC}$, and using the exogenously driven relationship $S_{NC} = \Delta EE_{NC}/(\Delta EE_{NC} + \Delta PE)$, the following expression, in conjunction with Eq. (26), can be used to establish $UC_{EI,NC}$ values used in the evaluation of the present value of abatement costs, PV_A:

$$UC_{NC} = (\beta/m)^{1/r_{NC}} (UC_{EI})^{\rho} \quad . \tag{28}$$

Along with β, ρ, and m(t), this share-based relationship for determining specific $UC_{NC,EI}$ values from the equi-preference "budget equation", Eq. (26), is also exogenously driven. Alternatively, $UC_{NC,EI}$ can be specified directly at time t_1, and then diminished with time by the factor $1/(1 + r_{TP}^{NC,EI})^{t-t_1}$ according to assumed technological progress rates, r_p^{NC} and r_p^{EI} (1/yr); results from both approaches to determining $UC_{NC,EI}$ are reported.

With $UC_{EI,NC}$ determined, the present value (referenced to 1995) of all mitigation costs associated with a given scenario is determined as follows:

$$PV_A(B\$) = \int_o^t \frac{UC_{NC}\ \Delta EE_{NC} + UC_{EI}\ \Delta PE}{(1 + r)^{t'}}\ dt \quad , \tag{29}$$

where $UC_{NC,EI}$ as used in this expression designates either the solution to Eqs. (27) and (28) or are technologically discounted initial values. The cost of abatement, PV_A, reflects cost incurred by improving efficiency and implementing (assumed more costly) NC generation technologies in place of schemes that utilize carbon-based fuels. It is emphasized that $UC_{NC,EI}$ values determined from an indifference curve lie along a somewhat *ad hoc* line of equi-preference/indifference [Eq. (26)], with specific combinations of the two being dictated by market- and policy-motivated choices [Eq. (28)]. Detailed bottom-up energy analyses could uncover connectivities with other sectors that in turn could lower or even reverse the sign of these abatement charges.[1,2] Also to be emphasized is the fact that the EI *versus* NC approaches to mitigating GHG accumulations and related effects are but two of a number of responses to the threat of greenhouse warming[5] (*e.g.*, reduce *per-capita*

energy consumption; offset effects through "climatic engineering"; both reactive and proactive adaptation to warmer/wetter climates).

The present value of the abatement cost, $PV_A(B\$)$, gives the discounted cost of abating CO_2 at time t. One measure of "benefit" accrued up to time t is the difference in the discounted values of GHG-related damage relative to the BAU (*e.g.*, t = 0) case, where,

$$PV_D(B\$) = \int_0^t \frac{H(t')}{(1 + r)^{t'}} \, dt' \ , \tag{30}$$

This expression is evaluated for both the BAU (non-driven) and the base (driven) case. An alternative measure of benefit accrued as a result of the expenditure PV_A is based on the present value of the product UC_D R; both measures are evaluated and compared to PV_A on a benefit-to-cost basis, with the latter being adopt in comparisons of parametrically varied results. In either case [*e.g.*, present value of cost damage function, (Eq. (30); or the present value of the marginal damage cost], the "cost" is taken as PV_A, and the "benefit" is computed as $\Delta PV_D = (PV_D)_{BAU} - (PV_D)_{BAS}$, where BAU is the t = 0 business-as-usual case and BAS is the (particular) base case under study.

IV. RESULTS

The results presented herein are preliminary and are intended primarily to provide an example for comment on the way to applications in larger models.[15,17] Two base cases are identified as BASE1 and BASE2, both of which derive from the parameters listed in Table I. The following subsection describes the results generated under the BASE2 conditions. As is indicated in Table III, the BASE1 and BASE2 cases represent respective points of departures for a series of overlapping parametric studies of the impact on GHG abatement and damage costs associated with the NC (increased use of Non-Carbon fuels for electricity generation) *versus* EI [decreased Energy Intensity (MJ/$) or increased end-use efficiency]. Along with examining the impacts of the rate of GPC increase (*e.g.*, T_{GPC}) and the share-fraction weights used to identify a point on the $UC_{NC,EI}(\$/GJ)$ indifference curve [*e.g.*, the ratio $\beta = b_{NC}/b_{EI}$, Eqs. (26) and (27)], the results from parametrically varying f_{NCf} and EI_f follow the report on BASE2 results. As is indicated on the Table-III

"roadmap", a case is considered that describes a "maximum abatement" scenario, wherein the driver functions use simultaneously the maximum f_{NCf} and EI_f considered in those respective parametric series. These computations are conducted for a ~100-year time horizon. Extending this time horizon to ~200 years, and using exogenous, discounted unit differential costs, $UC_{NC,EI}$, a series of final parametric studies examines both the impacts of $UC_{NC,EI}$ and the rate at which decreased energy intensities are achieved; as is indicated on Table III, these latter studies are referenced to BASE3 conditions, which are similar to those that define BASE2, except for the expanded time scale and the external input of $UC_{NC,EI}$.

A. Base Case

The BASE1 and BASE2 parameters are given in Table I; also listed are the business-as-usual (BAU) parameters used as a reference case to determine benefit-to-cost ratios. Figure 1 gives the time variation of exogenous drivers for the BASE2 conditions, as described in Sec. II.A.: f_{EE}, f_{NC}, α, EI, and GPC. The time dependence of the fractions EE_{NC}/PE, $(EE_{NC} + \Delta PE)/PE$, and $EE_{NC}/(EE_{NC} + \Delta PE)$ that result are given in Fig. 2, where EE_{NC} is the total non-carbon (electrical) energy demand, and ΔPE is the reduction in primary energy demand induced by decreased EI relative to the BAU case. The respective normalized rates, $\varepsilon_j(1/yr)$, are given in Fig. 3, and the time dependencies of PE and POP that results from the integration of ε_{PE} and ε_{POP}, along with GWP = GPC × POP, are given in normalized form on Fig. 4. These results are similar to results suggested as nominal by more elaborate models.[15,17] Figure 5 plots the magnitudes of PE(EJ/yr) and EE_{NC}(GWeyr/yr), for the BASE2 case (BAS), while also giving respective BAU values.

The evolution of atmospheric carbon emissions and accumulations is depicted in normalized form on Fig. 6 for these BASE2 parameters; the BASE2 average global temperature increase (computed from the base year t_o = 1800, following Ref. 18), ΔT, is also included on Fig. 6; on this figure, M(GtonneC) represents total integrated emission relative to W_o, whereas W(Gtonne) is the carbon associated with CO_2 actually retained in the atmosphere. A comparison of relative CO_2 accumulations, W/W_o, and ΔT between the BASE2 and the associated BAU cases is depicted on Fig.7. Figure 8 plots ΔT *versus*

W/W_o for the BASE2 case. The increasing accumulation of atmospheric carbon that accompanies the drive for increased human welfare, as reflected in the exogenously driven increase in GPC (\$/*capita*), is depicted explicitly in Fig. 9 for the BASE2 parameters. Also shown on this figure is the time evolution of the damage fraction, k_T [Eq. (22)], which is the fraction of the GWP at that time attributable to damage associated with greenhouse warming. The dependence of k_T on the fitting parameter ν is also shown; the point of common intersection for these k_T curves corresponds to the time when $\Delta T = T_{REF}$, according to Eq. (22).

Equations (8) and (9) are plotted in Fig. 10 for the BASE2 case driver functions (*e.g.*, EI/EI_o and f_{EE} f_{NC}). While for the BASE2 case the fraction of electrical energy provided by NC sources, f_{NC}, increases (Figs. 1 and 2), for the BASE1 case f_{NC} actually decreased with time, albeit EE_{NC} nevertheless increases. In the BASE1 case, the impact of energy efficiency on reducing atmospheric carbon emissions (which operates on all of PE) is far greater than for approaches based on application of NC sources. The BASE1 and BASE2 cases are adopted to reflect these differing points of departures in examining the importance of EI *versus* NC approaches to GHG abatement.

The present value of damage cost for the BASE2 case is shown on Fig. 11 for a range of EMUC [γ, Eq. (25)] and damage-function parameter [ν, Eq. (22)] values. Generally, increased EMUC values more strongly discount the future, leading to reduced present-value estimates of damages incurred from greenhouse warming. For a given γ, however, lower values of the parameter ν results in an increase in shorter-term damage costs, which contribute more to the present-valued sum than a damage function that scales with temperature to a higher power ν, albeit, that function later suggests greater longer-term costs. These remarks pertain to the present case, where: a) the parameters k_{REF} and T_{REF} in Eq. (22) are held constant; and b) human and/or ecological costs related to the rate of temperature increase (*e.g.*, inability to adapt, $k_{DT} = 0.0$) are not incurred. The wide variability of potential damage costs related to the interaction between the degree to which future costs are discounted and the temperature sensitivity of those costs, as expressed in terms of a fraction of GWP, is evident from Fig. 11.

The damage costs reported on Fig. 11 are derived from the present value of costs actually incurred at a given time [*e.g.*, Eq. (22)]. Figure 12 gives the present value of damage costs computed from the marginal cost of greenhouse-warming damage, UC_D, as given by Eq. (24). The damage cost computed in this way is used in parametric studies reported in the following subsection. A comparison between Figs. 11 and 12 indicated an even greater variability in PV_D for the latter as γ and/or ν are varied. The importance of "front loading" damage costs by using lower values of the damage cost function parameter ν is diminshed for PV_D computed from the marginal unit cost, UC_D. The cross-over of the PV_D curves in Fig. 12 for a given value of γ occurs at time when $\Delta T \simeq T_{REF}$, as described in conjunction with Fig. 9.

The "benefit" derived from any combination of NC and EI abatement schemes is defined as the difference in PV_D between the case being examined and the BAU case, as described above and defined in Table I. Generally, the BAU case is represented as little or no change in f_{NC} and EI from the initial conditions, f_{NCo} and EI_o. For the BASE1 case, f_{NC} actually decreases from the initial value. In either case, the "benefit" at any given time is defined as $\Delta PV_D = (PV_D)_{BAU} - (PV_D)_{BAS}$.

The "cost" of any NC/EI-based abatement scheme, PV_A, is the present value as describe by Eq. (29). These abatement costs are show for the BASE2 conditions on Fig. 13, which also indicates a strong variability with the values of γ and/or ν chosen. This ν variability is driven by the choice of $UC_{NC,EI}$ based on the indifference-curve/share-fraction algorithm [Eqs. (26) and (27)]; as is shown in Sec. IV.B.6., exogenous input of technologically discounted $UC_{NC,EI}$ values remove this ν dependence.

The "integrated" unit cost of damage computed simply as the ratio of PV_D and the total atmospheric carbon emission, M. The time evolution of this ratio is shown as a function of γ and ν in Fig. 14 for the BASE2 conditions. For the reasons cited above, the greater discounting for higher γ values leads lower integrated unit damage costs, as does larger values of the scaling exponent, ν. At earlier times, this behavior is scrambled for a unit cost of damage expressed as the simple ratio PV_D/M. An economically more appropriate unit

damage cost is the marginal unit damage cost, UC_D, given by Eq. (24) and used to compute the PV_D values in Fig. 12. As noted previously, this value is used to compute the present value of damage cost, PV_D, for all subsequent parametric studies. Figure 15 gives the γ - and ν-dependence of this UC_D time evolution.

Before the cost of NC/EI-base CO_2 abatement (Fig. 13) can be computed, specific values of $UC_{NC,EI}$(\$/GJ) are required. As described in Sec. II.B., rather than choose specific values for these incremental unit costs, the time-evolving (*e.g.*, UC_D) indifference curve given by Eq. (26) is used. These linear relationships are displayed in logarithmic form on Fig. 16 for a range of ν values and $\gamma = 1$. Also shown are the share-fraction constraints, Eq. (27), for three values of the NC/EI weight ratios, $\beta = b_{NC}/b_{EI}$; the BASE1 and BASE2 conditions correspond to $\beta = 1$. The time evolving $UC_{NC,EI}$ are determined from the intercepts of these indifference and share-fraction relationships, from which the present value of the cost of abatement, PV_A(T\$), is determined. Results based on exogenously determined $UC_{NC,EI}$ values are described in Sec.IV.B.6. with respect to BASE3 conditions (Table III).

With the "benefits", ΔPV_D, and the "costs", PV_A, of abatement *vis à vis* NC and EI routes determined, a benefit-to-cost ratio can be formed. The time evolution of this ratio is given on Fig. 17 for a range of γ [E_{MUC}, Eq. (25) and ν [damage cost function, Eq. (22)] values. Generally, both ΔPV_D and PV_A increase with time, with the direct impact of discounting (*e.g.*, γ) being considerably reduced in importance when the benefit-to-cost ratio, $\Delta PV_D/PV_A$ is formed. The chief impact is through the damage function scaling parameter ν. As noted above, the concave-downward dependence of damage cost on temperature increase when ν is less than unity "front loads" this costs in the present-value process, in spite of the lower costs such a function projects in the longer term (for the same values of k_{REF} and T_{REF}). Consequently, time discounting, at whatever level, favors lower present-valued damage costs for $\nu > 1$, albeit such a functional dependence of damage costs on temperature rise projects larger costs in the out years. This concavity

effect on P_D occurs for ΔT values below T_{REF}, as is indicated by the dependence of k_T on ν given on Fig. 9. For times where ΔT exceeds T_{REF}, higher ν values give higher PV_D costs, with the "benefits" $\Delta PV_D = (PV_D)_{BAU} - (PV_D)_{BAS}$ being larger for larger values of ν at later times. The behavior reported on Fig. 17 is further complicated by the ν-dependence of the unit differential costs, $UC_{NC,EI}$, as determined from the indifference-curve/share-fraction algorithm (Fig. 16). Section IV.B.6. elaborates on these interactions, which become ever more convolved when $UC_{NC,EI}$ are exogenously determined.

B. Parametric Cases

The results of a series of two primary (*e.g.*, f_{NCf} and EI_f) and two subsidiary (*e.g.*, T_{GPC} and $\beta = b_{NC}/b_{EI}$) parametric variations are reported in this section in relationship to the BASE1 and BASE2 conditions. Extending the computational time horizon from 100 to 200 years and using exogenous $UC_{NC,EI}$ values, a BASE3 case is defined against which variations in the time scale of EI decreases, T_{EI}, are studied. In "roadmap" form, Table III describes these variations: a) variation of f_{NCf} (Cases 1-4, with Case 1 identified as BASE1 and Case 2 identified as BASE2, as is reported in the previous section); b) variation of EI_f, (Cases 1, 4, and 5); variation of *per-capita* GWP growth rate, T_{GPC} (Cases 2, 7, and 8); and d) variation of the NC/EI share-fraction weighting ratio, $\beta = b_{NC}/b_{EI}$ (Cases 2, 9, 10). The stand-alone Case 11 is identified as a "maximum abatement" case, where f_{NCf} and EI_f are set at the maximum of the respective ranges examined in the aforementioned parametric surveys. Cases 12 $\rightarrow$ 15 examine the impact of exogenous changes in $UC_{NC,EI}$, which discount for technological progress at rates $r_{TP}^{NC} = r_{TP}^{EI} = 0.01$ 1/yr; the BASE3 case is similar to BASE2 and is identified as Case 15. In reference to BASE3 conditions, the impact of varying the time scale, T_{EI}, over which improvements in EI are implemented is examined in the series Cases 16 $\rightarrow$ 18.

1. Non-Carbon (Electrical) Energy Generation

The impact on atmospheric carbon emission rates and accumulations for the f_{NCf} variation are shown on Fig. 18. Increased NC generation (Cases 1 → 2 → 3 → 4) decrease CO_2 emissions, accumulations, and associated temperature increases. The upper limit of $f_{NCf} = 0.9$ is considered as extreme and could reduce the 100-year emission rate by over a factor of two, which leads to a reduction in atmospheric CO_2 concentration of ~60% (relative to the BAU $f_{NCf} = 0.1$ case); the resulting 100-year temperature rise is reduced by ~70%. The impact on the required EE_{NC} annual generation for this range of f_{NCf} values is shown on Fig. 19. Even for the $f_{NCf} = 0.6$ case, the build rate for these NC electrical generation systems, for a capacity factor of $p_f = 0.75$, amounts to ~ 130 GWe/yr.

For $\nu = 1$ and $\gamma = 1$, the time evaluations of the damage and abatement costs, PV_D and PV_A, respectively, are shown as a function of f_{NCf} on Fig. 20; for most cases, the present value of abatement exceeds the present value of damage after ~50 years for $\nu = 1$ and $\gamma = 1$. As described above, the "benefit", $\Delta PV_D = (PV_D)_{BAU} - (PV_D)_{BAS}$, is defined in relationship to the BAU case; Fig. 21 gives the ratio $\Delta PV_D/PV_A$ as a function of time and ν for $\gamma = 1$, where the γ dependence was shown to be weak (Fig. 17) for $UC_{NC,EI}$ determined according to the Eqs. (26) - (27) indifference-curve/share-fraction algorithm. Generally, for the share-fraction weights used ($\beta = 1$), benefit-to-cost ratios above unity are possible only for damage functions that do not load damage costs to heavily into periods where they appear too large in the present-value sums. Values of $\nu \gtrsim 1$ are "desirable" in this regard.

2. Energy Intensity

The effects on CO_2 emission rates, atmospheric accumulations, and related temperature increases as the energy-intensity goal is varied above and below the BASE1 (and BASE2) value of 10 MJ/$ are shown on Fig. 22; increased efficiency (Cases 5 → 1 → 6, Table III) decrease emissions even more than increased use of NC fuels for electricity generation. Interpolating the Fig.-22 results suggests that emissions can be stabilized at roughly twice

present values if $EI_f \simeq 7$ MJ/$ could be achieved. The limit of $EI_f = 5$ MJ/$, which is approached on the assumed $T_{EI} = 60$-yr time scale, would lead to a doubling of the atmospheric CO_2 concentration, and a somewhat large factor of increase in average global temperature by ~ 2100. The impact of this range of goal-EI values on primary and non-carbon annual energy demand is depicted on Fig. 23, with Fig. 24 giving the time evolution of the present value of damage and abatement costs for $\nu = 1$ and $\gamma = 1$. The realism of the $EI_f = 5$ MJ/$ case, particularly in view of the large decreases in *per-capita* energy consumption required to accompany the (driven) increased *per-capita* GWP, is questioned; this issue is addressed further in Sec.IV.B.7., where the EI improvement time scale, T_{EI}, is varied. For the EI approach to CO_2 mitigation, these abatement costs do not exceed the damage costs until times ~ 100 years. Although the general trends are similar to the NC variations, when expressed on a benefit-to-cost basis, the time evolution of the ratio $\Delta PV_D/PV_A$ and the dependence on ν (again, $\gamma = 1$) shown on Fig. 25 for the EI parametric series is more complex, although the general trends with increasing ν discussed above apply for any given value of EI_f. Generally, in terms of these benefit-to-cost ratios, increasing energy efficiency (decreasing EI_f) and increasing ν (larger damaged costs pushed farther into a discounted future) are "good".

3. Rate of *per-capita* GWP Increase

The impact of delaying the rate at which human economic welfare is improved on atmospheric carbon accumulations is driven in this model by the feedback assumed between population growth and GPC [Eq. (7)]. Figure 26 gives the time dependence of relative population, primary energy demand, and GWP as T_{GPC} is varied above the BASE1 and BASE2 values (Table III, Cases $2 \rightarrow 7 \rightarrow 8$). Population growth is increased, but the use of less energy by these less-improved populations is reduced; total GWP initially slackens, but even at the lower *per-capita* GWP, total GWP is pushed upward by the growing population. The resulting impacts on CO_2 emission rates, accumulations, and associated temperature rise is shown on Fig. 27. Lastly, the relationship between relative accumulated atmospheric carbon on the relative *per-capita* GWP improvement is shown on Fig. 28 for this series of delayed GPC improvement rates (Cases $2 \rightarrow 7 \rightarrow 8$), along with the previously reported f_{NCf} and EI_f series. Each curve on Fig. 28 terminates at 100 years.

The delayed GPC improvement cases have the highest carbon accumulation for a given level of *per-capita* GWP improvement (*i.e.*, reduced T_{GPC}). Each extreme for the f_{NCf} and EI_f cases (*e.g.*, $f_{NCf} = 0.9$ for $EI_f = 10$ MJ/$ or $EI_f = 5$ MJ/$ for $f_{NCf} = 0.3$) projects the highest *per-capita* increase for the lowest increase in atmospheric CO_2 concentration; the combination of these f_{NCf} and EI_f extrema into the "maximum abatement" Case 11 is also included on Fig. 28.

4. Supply-Side *versus* Demand-Side Share-Fraction Weights

Figure 16 gives the impact on the choice of the differential unit costs for NC and EI abatement, $UC_{NC,EI}$($/GJ), along any given indifference curve, as described by Eq. (26), when the relative weights, $\beta = b_{NC}/b_{EI}$, are shifted from the BASE1/BASE2 value of 1. The impacts of these shifts on the benefit-to-cost ratio for $\gamma = 1$. and a range of ν values are depicted on Fig. 29 for the BASE2 conditions. As previously noted, the time evolution of the share fraction *per se* is determined by the driver functions (Fig. 1). For reasons discussed previously, damage cost functions described by higher temperature-rise exponent give higher benefit-to-cost ratios earlier. For a given ν value, this "desirable" condition is achieved if $\beta > 1$ (*e.g.*, a stronger weighting is given to the NC route to abatement).

5. Maximum Abatement Case

Case 11 listed in Table III describes a combination of the most optimistic limits considered separately in the respective NC and EI parametric studies. The impact on relative CO_2 accumulation and associated temperature rise is shown on Fig. 30 in relationship to the BAU case when these f_{NCf} and EI_f extrema are combined. Comparisons on the W/W_o *versus* GPC/GPC_o "phase space" of this "maximum abatement" case with previously reported f_{NCf}, EI_f, and β parameteric variations are given on Fig. 28. Lastly, the time variation of the benefit-to-cost ratio and the dependence on γ and ν are shown on Fig. 31 for this case.

6. Exogenous NC and EI Unit Differential Costs

a. The BASE3 Case

All parametric results presented up to this point have used the indifference- curve/share-fraction algorithm [Eqs. (26) and (27)] to select the NC and EI unit differential costs, $UC_{NC,EI}$(\$/GJ), need to compute the present value of the abatement cost, PV_A(T\$). Furthermore, computations so far extend only to a 100-year time horizon to the year ~2100. The present section exogenously (and parametrically) specify these unit differential costs to equal some initial value $UC_{NC,EI}$ that is decreased in time by a technological progress factor, $1/(+ r_{TP}^{NC,EI})^t$, where the technological progress factor is taken to be $r_{TP}^{NC,EI} = 0.01\ 1/\mathrm{yr}$. Furthermore, to facilitate an investigation of the impact of changing the time scale over which decreases in EI would be implemented, T_{EI}(yr), the time period of the computations are extended 200 years to ~2200. Lastly, the derivative $d\Delta T/dW$ used in Eq. (23) to evaluate the marginal cost function, $h(t,t')$, up to this point was computed by numerically differentiating the computed T *versus* W dependence; this procedure proves inaccurate/unphysical at longer times under (extreme) conditions where growth trends in ΔT and W may reverse; an (still approximate) analytic determination of $d\Delta T/dW$ is used in the following extended-time evaluations.

With these changes (*i.e.*, exogenous $UC_{NC,EI}$ with exogenous technical progress; extended time frame; and analytic $d\Delta T/dW$), the BASE2 reference condition given in Table III becomes a new BASE3 reference case. Figure 32 gives the time evolution of the present-valued damage costs, PV_D, for a range of γ and ν values. These results are similar to those reported in Fig. 12 for the BASE2 conditions. Higher rates of discounting (*e.g.*, the EMUC, the negative of which is modeled by γ) give lower present value of damage cost. The interplay between the damage-cost scaling parameter, ν, remains as reported earlier; for temperature rises below T_{REF}, k_T, and, hence, damage cost, increase for smaller values of ν, with this trend reversing once the ΔT exceeds T_{REF} (Fig. 9). As will be discussed, this

behavior couples with the level of discounting [Eq. (25)] to explain the interplay of the benefit-to-cost ratio with these parameters.

The present-value of the abatement charges given for BASE3 conditions in Fig. 33 expectedly differs both in form and in the absence of ν-dependencies from the counterpart BASE2 behavior depicted in Fig. 13. The marginal unit damage costs given in Fig. 34 as a function of time, ν, and γ are similar to those reported earlier in Fig. 34, with slight differences reflecting largely the change in the means by which $d\Delta T/dW$ in Eq. (23) is estimated. Driven primarily by changes in PV_A magnitudes, and dependencies on γ and ν, significantly different t-γ-ν dependencies depicted for the benefit-to-cost ratio, $\Delta PV_D/PV_A$, on Fig. 35 result. To understand the interactions between ν and γ in setting the relative $(PV_D)_{BAU}$ and $(PV_D)_{BAS}$ time dependencies depicted on Fig. 35, it is recalled that "benefit, $\Delta PV_D = (PV_D)_{BAU} - (PV_D)_{BAS}$, is the difference between the BAU and the BAS cases. Larger values of ν give larger values of $(PV_D)_{BAU}$, and, for the conditions that define the BAS condition, the benefits of moving off the BAU case are greater. These larger benefits are sustained for cases that are not heavily discounted (*e.g.*, low γ values), in spite of the fact that the abatement costs, PV_A, that form the denominator of the "benefit-to-cost" ratio is also larger for smaller γ values. The interlaced behavior at earlier times indicated on Fig. 35 for the same γ results from the previously described concavity behavior as temperature rise approaches and then surpasses T_{REF} for a given value of ν (*i.e.*, k_T in Fig. 9).

The behaviors summarized on Figs. 32-35 mirror those reported for the BASE2 case on Figs. 1-17. The conditions describe above and elaborated on Figs. 32-35 define the BASE3 conditions against which subsequent impacts of variations in $UC_{NC,EI}$ and T_{EI} are referenced.

b. Unit Differential Cost Variations

As is indicated on Table III, $UC_{NC,EI}(\$/GJ) = \eta_{TH}\ \Delta COE_{NC,EI}/3.6$, was varied of the range $\Delta COE_{NC,EI} = 10 \rightarrow 20$ mill/kWeh. The impact of these extrema on the present value of the abatement costs, PV_A, is shown on Fig. 36 for $\nu = 1.0$ and three values of the negative EMUC, γ; as expected, increasing γ(discounting) and decreased $\Delta COE_{NC,EI}$ results in lower PV_A trajectories. The strong impact of these $\Delta COE_{NC,EI}$ variations (again, $r_{TP}^{NC,EI} = 0.01$ 1/yr for all cases) on the benefit-to-cost ratio is shown on Fig. 37. In terms of the benefit-to-cost ratio $\Delta PV_D/PV_A$, increased discounting (γ), which for the reasons discussed above push benefit-to-cost to later times (Fig. 35) for exogenously determined unit differential costs, can be counteracted by decreases in the (starting) unit differential costs, $UC_{NC,EI}(\$/GJ)$.

7. Rate of Energy Intensity Decrease

As discussed in Sec. III.A., four exogenous rates drive this model. In terms of the respective e-folding times, these time scales are determined by: a) the time for EI decrease, T_{EI}; the time for decrease in the carbon coefficient for the fossil fuels being used, T_α; c) time scale for increased electrification of the primary energy demand, T_{EE}; and d) the time scale over which the fraction of the demand EE provided by non-carbon fuels is increased, T_{NC}. Lastly, central to this model is the time scale T_{GPC} over which the *per-capita* GWP is increased. Section IV.B.3. examined the impact of changes in T_{GPC}. Although the goal fractions $f_{EE} = EE/PE$ and $f_{NC} = EE_{NC/EE}$ are important drivers (Sec. IV.B.1.), as is the goal value for energy intensity, EI_f (Sec. IV.B.2.), the primary rate sensitivity of greenhouse-warming (economic) impacts is exerted through T_{EI}, since f_{NC} operates only on a small part of total energy demand for any "realistic" limits imposed on f_{EEf} and/or f_{NCf} (and EE_{NC} implementation rate). This section reports on the impact of decreases in the EI time scale, T_{EI}.

The time trajectories of PE(EJ/yr) and EE_{NC}(GWe yr/yr) are shown in Fig. 38 for a range of T_{EI} values for what are otherwise BASE3 conditions; the $T_{EI} = 60$-yr case corresponds to the BASE2 case. The driver model used in this study determines the PE growth rate,

ε_{PE}, *vis à vis* Eq. (6): $\varepsilon_{PE} = \varepsilon_{EI} + \varepsilon_{GPC} + \varepsilon_{POP}$. As time advances, the GPC and POP rates diminish, and, depending on the value of T_{EI} (ε_{EIo} $T_{EI} = EI_f/EI_o - 1$), the negative ε_{EI} can dominate, thereby driving a decrease in PE at later times. For the lower values of T_{EI} considered, *per-capita* energy consumption, EPC(GJ/*capita*), at later times can fall below present levels. This behavior is illustrated in Fig. 39; based on EPC consideration, values of T_{EI} below ~40 years, for the other constraints imposed (Sec. III.A.), are considered unrealistic.

The associated impacts on CO_2 emission rates, R(Gtonne/yr); CO_2 accumulations, W(Gtonne); and associated temperature rise, $\Delta T(K)$, are depicted on Fig. 40. For these BASE3 conditions with T_{EI} decreased to ~40-50 years, the rates of carbon emission return to present levels in ~200 years, with an asymptotic increase in CO_2 concentration of 2.5-3.5 over pre-industrial (t_o = 1800) values and a global warming of $\Delta T \gtrsim 3$ K. The dependence of the environmental *versus* economic welfare on T_{EI} is shown on Fig. 41, which quantifies the reduced CO_2 accumulations for a given increase in *per-capita* GWP as T_{EI} is reduced. As noted above, consideration of EPC limitations indicate that $T_{EI} \lesssim 40$ yr lead to unrealistic expectations for the constraints imposed (Sec. III.A.).

The present value of (NC + EI) abatement costs are shown as a function of time on Fig. 42 for these T_{EI}-varying BASE3 condition and for a range of negative EMUC values; discounting reduces costs, and accelerated implementation of EI methods for a given discount rate increase costs. While these results for the BASE3 conditions are independent of the parameter ν, the present values of damage costs, PV_D, are not. Figure 43 gives the time evolution of PV_D as a function of γ for $\nu = 1.0$ (damage costs ~ ΔT). As for PV_A, increased discounting reduces damage costs, as does more rapid implementation of schemes for decreasing EI. As was indicated for a range of target variations performed under the BASE2 conditions, the dependence of the benefit-to-cost ratio of T_{EI} is negligible; this behavior is shown on Fig. 44 for $\nu = 1$ and a range of γ values. The more attractive benefit-to-cost ratios occur for a less-discounted situation for the reasons given in explaining Fig. 37; higher values of this ratio are favored by the larger benefits,

$\Delta PV_D = (PV_D)_{BAU} - (PV_D)_{BAS}$, retained by not discounting heavily, in spite of the higher present value of abatement costs.

V. SUMMARY AND CONCLUSIONS

A simplified, exogenously driven model of global energy demand has been evaluated to examine the connection between the aggregated human economic welfare parameter, GPC($/*capita*), and the accumulation of greenhouse-warming gases in the atmosphere for a range of supply-side (NC electricity generation, $f_{EE}f_{NC}$) and demand-side (energy efficiency, EI) drivers. While the latter, when applied to the full spectrum of PE demands, is expectedly much more effective in reducing carbon emission for a given GPC goal (*e.g.*, the attainment of a final value GPC_f on a given time scale, T_{GPC}), displacement of atmospheric carbon sources through implementing NC electrical generation can also be important. The relative CO_2 emission rates, R/R_o, atmospheric accumulations, W/W_o, and average temperature increases, ΔT, that result from increases in the fraction of electrical energy derived from NC sources (f_{NCf}, Fig. 18), decreases in energy intensity (EI_f, Fig. 22), and the combination of the more optimistic limits of the two ("maximum abatement", Fig. 30) have been collected and compared on Fig. 45. Interestingly, even though the NC abatement approach operates only on electrical energy (EE, which for all cases is assumed asymptotically to achieve $f_{EE} = 0.6$ of total primary energy, in equivalent units, on a T_{EE} = 20-yr time scale), the extreme case of $f_{NCf} = 0.9$ is slightly more effective in mitigating CO_2 accumulations and temperature rise than the limiting case where $EI_f = 5$ MJ/$ (f_{NCf} in this case is fixed to the BASE1 value of 0.1); the timescale for application of the NC *versus* the EI remedy is crucial. Figure 45 also gives the respective trajectories for the highly optimistic "maximum abatement" case, where $f_{NCf} = 0.9$ and $EI_f = 5$ MJ/$.

Estimates of present value costs of damage and abatement, PV_D and PV_A, respectively, are sensitive to: a) whether the damage cost function [Eq. (22)] or the marginal unit cost of damage [Eq. (24)] is used (*e.g.*, Figs. 11 *versus* 12); b) the concavity of the relationship assumed between damage cost and temperature rise [the exponent ν in Eq. (22) for given values of k_{REF} and T_{REF}); c) the value of the elasticity of marginal utility of consumption, γ [Eq. (25)]; and d) the procedure used to select the unit costs abatement, $UC_{NC,EI}$($/GJ), where either the latter is specified outright, or is selected from an indifference curve

[Eq. (26)] for a given (logit) relationship between the (exogenously driven) share fraction and the respective unit costs [Eq. (27)]. Using the indifference/share-fraction relationships to determine $UC_{NC,EI}$, generally large reductions in the damage cost, $\Delta PV_D = (PV_D)_{BAU} - (PV_D)_{BAS}$, are accompanied by large abatement charges, PV_A. The extent to which a benefit-to-cost ratio, $\Delta PV_D/PV_A$, can achieve values above unity within the 100-year time frame is strongly determined by the values of the damage cost function scaling parameter ν; the strong dependence of PV_D and PV_A on the EMUC, γ, largely disappears upon formation of this benefit-to-cost ratio. Generally, larger values of ν supress early damage cost in the present-worth computation, but enhance later costs, particularly for the BAU case against which the "benefit" ΔPV_D is measured. Depending on the means by which the differential unit costs of abatement, $UC_{NC,EI}$, are determined, a complex time-dependent dependence of the resulting "benefit-to-cost" ratio results that generally favors higher value of ν (Figs. 17 and 35). These ratios are relatively independent of γ for $UC_{NC,EI}$ values chosen from the indifference curves (Fig. 17), but favor lower values of γ when $UC_{NC,EI}$ are specified exogeneously (*i.e.*, reduced discounting of "benefits," ΔPV_D, in spite of less discounting of costs, PV_A).

For the "optimistic" $\nu = 2.0$ scaling (*e.g.*, higher costs incurred at later times are reduced by the discounting procedure), the time evolution of these benefit-to-cost ratios for both the BASE2 f_{NCf} and the BASE1 EI_f parametric series are compared on Fig. 46; the "maximum abatement" case is also shown, as is the case where $\beta = b_{NC}/b_{EI}$ is increase from unity to ten. Within the constraints imposed in generating the Fig.-46 comparison, and excluding the $EI_f = 15$ MJ/$ case as being too close to the BAU case, the benefit-to-cost ratios are surprisingly similar, irrespective of the (NC *versus* EI) abatement scheme.

While this assessment of relative costs of supply-side (NC) *versus* demand-side (EI) GHG abatement indicates little potential cost advantage of one over the other, for different reasons, however, both may present serious problems of implementation, at least in the short term. The "maximum abatement" limits of $f_{NCf} = 0.9$ and/or $EI_f = 5$ MJ/$, both achievable with time constants of $T_{NC,EI} \sim 60$ yr, represent formidable achievements: total

capitalization of the former and bottom-up implementation at the indicated unit costs for the latter.

Lastly, for the simplified model used to couple population growth to GPC growth, environmental penalties in the form of increased accumulations of atmospheric carbon accompany delays in increasing the aggregate "human welfare" parameter, GPC. Figure 28 indicates the long-term environmental penalty of reducing the rate of GPC increase in the form of a "phase space" defined by GHC accumulations *versus* improved welfare parameter, GPC/GPC_o; this figure, along with the T_{EI} variations given in Fig. 41, compares key sensitivity studies reported herein.

The primary purpose of this exogenously driven, globally aggregated model is to examine trade offs associated with supply-side (NC) *versus* demand-side (EI) approaches to CO_2 abatement under conditions that couple *per-capita* economic growth to population growth. The full execution of this model required certain *ad hoc* assumptions to be made that otherwise would not be necessary (or at least would be better camouflaged) by the use of a detailed bottom-up or top-down model. In spite of the weak costing bases (particularly for demand-side abatement schemes), the "market-free" character, and the high degree of aggregation of this model, the following "top-level" interim findings emerge:

- The "battle of rates" between atmospheric processes, societal betterment, technology innovation/diffusion/implementation, and the economics and ethical forces of future discounting, not to mention the kinetics of human adaptability, clouds any prescriptions for direct action on a perceived problem that may or not turn out to be real;

- If tolerances for achievable limits on asymptotic limits for f_{NCf} and EI_f can be expanded, either approach has much to offer;

- If population growth is in fact tied to *per-capita* GWP, much in terms of reduced CO_2 emissions for a given achievement in *per-capita* GWP can be gained by not delaying GPC growth; a similar comment applies to the rate at which EI is decreased.

- Significant reductions in greenhouse-warming damage costs are accompanied by significant abatement costs for either supply-side (NC) or demand-side (EI) abatement approaches; the ratio of the benefits of reduced damage costs (relative to essentially "do nothing" BAU scenario) to the costs of abatement is:

  - highly sensitive to the scaling of the damage cost function with temperature rise and to the discounting procedure, even for a zero rates of pure time preference;
  - relatively insensitive to the (EI *versus* NC) abatement scheme.

In concluding, two generic comments are made that are applicable to both this simplified model as well as other more-detailed models of energy-economic-environmental interactions. This "market-free" model, as well as detailed top-down market equilibrium models,[8,15] are characterized by two potentially serious shortcomings: a) reliance on highly aggregated, exogenously input measures of human development (*e.g.*, GPC in this model or regional population and GWP growth rates in more detailed models); and b) exogenous accommodation of non-price improvements in the (efficient) use of energy [*e.g.*, EI(t) in this model or AEEI (or the equivalent) in more detailed analyses].

Human Welfare and GNP *per capita*: The use of an aggregated measure of *per-capita* GNP (or GWP, in the case of this analysis) tacitly assumes that growth in GPC contributes to a general rise in the living standards of the aggregated persons. The pitfalls of this equating of "growth" to "development" is elaborated in Ref. 25, which gives instances of strong growth with little development in the context of improved human welfare. A country GDP can grow rapidly with only a small proportion of the population benefiting from that growth; income distribution is a key issue that is easily lost in the aggregation process leading to the GPC metric. A number of considerations limit the accuracy of GPC as a measure of human welfare:[25] a) relative growth rates of GNP and population; b) distortions in relating real income and consumption data from a given country or region through some floating exchange rate that may not accommodate price parity mismatches; c) GNP growth without development in countries with strongly "dual" societies that translate into strong class distinctions and related inequities; and d) limitations of economic (monetary) consumption as a sole quality-of-life metric *versus* the use of important non-

monetary metrics (*e.g.*, education and literacy rates; infant mortality rate; life expectancy; *per-capita* consumption of calories, energy, meat, steel, durables, *etc.*) and/or related human development indices.[25]

Exogenous Non-Price Efficiency Improvements (EI, AEEI): This model, like more-detailed approaches,[8,15] input improved energy efficiency through the parameter ε_{EI} (or AEEI[8]) to effect non-price-induced reductions in energy use (and GHG emissions) per unit of productivity (GDP, GWP). Econometric models that divide regional economies into sectors[26,27] (*e.g.*, Coal Mining, Crude Oil and Gas Extraction, Electric Utilities, Gas Utilities, Petroleum Refining, Other Mining, Agriculture/Fishing/Hunting, Forestry and Wood Products, Durable Goods Manufacturing, Non-Durable Goods Manufacturing, Transportation, and Services, in the case of Refs. 26,27), and then specify differential rates of sectoral productivity growth for the same average labor productivity and population growth, can impress similar decreases in EI with ε_{EI} (or AEEI) equal to zero. Recent studies[26] have shown that reductions in EI are possible through differential rates of sectoral productivity growth, wherein average labor productivity and population growths are the same. Differential capital accumulations across sectors and strong growth in non-energy sectors (*e.g.*, the last seven of the twelve listed above) can increase the demand for energy, raise the price of energy, draw resources into the energy sectors, and lead to substitution away from energy inputs and into production. As noted in Ref. 26, the aggregate GDP growth rate can decrease with this reallocation of inputs, and the EI can decrease, thereby giving the appearance of an AEEI, albeit, this result is not driven by technological changes in energy use *per se*; changing patterns of energy demand are driven by differential (cross-sectoral) productivity growth.

Energy use and associated greenhouse-warming consequences are impacted strongly by both AEEI and GPC rates. Differential growth across sectors can be important in setting long-term GHG emissions and in identifying potential abatement scenarios. The applicability of economic models that directly or indirectly relate key drivers (*e.g.*, population growth, productivity growth, AEEI profile, tax rates, monetary policies, shifts in fiscal and other spending patterns, *etc.*) of GHG emissions to the future behavior and conditions/states of regions and economic systems that are potentially strong GHG sources must also be better understood in the context of these developing economies.[25] While

transparency in use and result remain as essential features of models used for generating scenarios of E^3 interactions and possible consequences, thereby limiting direct resolution of these multi-sectoral and multi-cultural issues, recognition and understanding of these limitations are important.

NOMENCLATURE

$A_j^{T,W}$	amplitude fitting coefficient for $R_{T,W}$
AEEI	autonomous energy efficiency improvement[8]
BAU	business-as-usual case designator
C(B$)	level of consumption
CGCM	coupled global climate model
PV_A(B$)	present value of abatement cost
PV_D(B$)	present value of damage cost
EE(EJ/yr)	electrical energy demand (thermal equivalent)
EE_{NC}(EJ/yr)	NC electrical energy demand (thermal equivalent)
EI(MJ/$)	primary energy intensity, PE/GWP
$EI_{o,f}$(MJ/$)	initial (final) primary energy intensity
EMUC	elasticity of marginal utility of consumption
EPC(GJ/*capita*)	primary energy per *capita*
e(GtonneC/yr)	CO_2 emission rate, same as R
f_{EE}	electric energy fraction (of PE)
$f_{EEo,f}$	initial (final) electric energy fraction
f_{NC}	NC electric energy fraction
$f_{NCo,f}$	initial (final) NC electric energy fraction
GHG	greenhouse gas
GNP(T$)	gross national product
GPC($/*capita*)	GWP *per capita*
GWP(T$)	gross world product
k_T	damage cost as fraction of GWP
k_{REF}	damage cost function parameter
H(B$)	damage cost function
h(B$/GtonneC/yr)	marginal cost function
LIRCM	linear integral response climate model[18]
NC	non-carbon energy source
PE(EJ/yr)	primary energy demand
PE_o(EJ/yr)	initial primary energy demand
POP(B)	population
POP_o(B)	initial population
R(GtonneC/yr)	atmospheric carbon emission rate
R_o(GtonneC/yr)	initial atmospheric carbon emission rate
$R_T(t-t')$	temperature impulse response function (K/GtonneC)
$R_W^*(t-t')$	temperature impulse response function (K/GtonneC) operating on dW/dt
$R_W(t-t')$	inventory impulse response function (unitless) operating on e(GtonneC/yr)
REF	reference case designator
r(yr)	discount rate
r_o(yr)	pure time preference
r_{TP}^j (1/yr)	rate of technological progress, (j = NC,EI)
t(yr)	time
$t_j^{T,W}$(yr)	exponent fitting coefficient for $R_{W,T}$

$\Delta T(K)$	average global temperature rise
$T_{REF}(K)$	global temperature rise where $k = k_{REF}$
$T_j(yr)$	characteristic time for evolution of parameter j
$UC_{EI,NC}(\$/GJ)$	EI (NC) carbon displacement unit cost
$UC_D(\$/tonneC)$	marginal damage cost
u(C)	utility of consumption at level C
vppm	volume parts per million
W(Gtonne)	global atmospheric CO_2 carbon inventory
$\alpha(Mtonne/EJ)$	carbon emission coefficient
$\alpha_{o,f}(Mtonne/EJ)$	initial (final) carbon emission coefficient
β	NC *versus* EI logit share weights, b_{NC}/b_{EI}
γ	elasticity of marginal utility consumption (EMUC), $u''(C)/u'(C)$
$\Delta COE_{EI,NC}(mill/kWeh)$	EI (NC) carbon displacement cost
$\Delta R_{EI,NC}(GtonneC/yr)$	carbon displaced by EI (NC)
$\Delta EE_{NC}(EJ/yr)$	electrical energy generated by NC sources relative to BAU case
$\Delta PE(EJ/yr)$	primary energy displaced by $EI < EI_o$, relative to BAU case
$\varepsilon_j(1/yr)$	normalized (logarithmic) rate for parameter j
ν	damage cost function parameter
ρ	ratio of EI and EC price elasticities, r_{EI}/r_{NC}, or ratio $\Delta COE_{NC}/\Delta COE_{EI}$.
$\tau_{CO_2}(yr)$	CO_2 matching coefficient between times t_o and t_1.

REFERENCES

1. M. Grubb, "Policy Modeling for Climate Change," Energy Policy, **21**(3), 203 (1993).

2. D. Wilson and J. Swisher, "Exploring the Gap: Top-Down *versus* Bottom-Up Analyses of the Cost of Mitigating Global Warming," Energy Policy, **21**(3), 240 (1993).

3. A. Manne and R. Richels, "Buying Greenhouse Insurance," Energy Policy, **19**(6), 543 (1991).

4. W. Nordhaus, "Count Before You Leap," The Economist, 19 (July 7, 1990).

5. W. Nordhaus, "To Slow or Not to Slow: The Economics of the Greenhouse Effect," The Economic Journal, **101**, 929 (1991).

6. S. C. Peck and T. J. Teisberg, "CETA: A Model for Carbon Emissions Trajectory Assessment," The Energy Journal, **13**(1), 55, (1992).

7. T. M. L. Wigley, R. Richels, and J. A. Edmonds, "Economic and Environmental Choices in the Stabilization of Atmospheric CO_2 Emissions," Nature, **379**, 240 (1996).

8. A. S. Manne and R. G. Richels, Buying Greenhouse Insurance: The Economic Costs of Carbon Dioxide Emission Limits, The MIT Press, Cambridge, Massachusetts (1992).

9. A. B. Lovins and H. L. Lovins, "Least-Cost Climatic Stabilization," Annual Review of Energy and Environment, **16**, 433 (1991).

10. R. H. Williams, "Low-Cost Strategies for Coping with CO_2 Emission Limits," The Energy Journal, **11**(3), 35 (199?).

11. J.C. Hourcade, "Modelling Long-Run Scenarios: Methodology Lessons from a Perspective on a Low CO_2 Intensive Country," Energy Policy, **21**(3), 309 (1993).

12. T. Barker, S. Baylis, and P. Madsen, "A UK Carbon/Energy Tax: the Macroeconomic Effects," Energy Policy, **21**(3), 296 (1993).

13. G. A. Goldstein, "MARKAL-MACRO: A Methodology for Informed Energy, Economic, and Environmental Decision Making," Brookhaven National Laboratory report BNL-61832 (May 16, 1995)

14. S. Messner and M. Strubegger, "User's Guide for MESSAGE III," International Institute for Applied Systems Analysis report WP-95-69 (1995).

15. J. Edmonds and J. M. Reilly, Global Energy: Assessing the Future, Oxford University Press, New York, NY (1985).

16. B. Keepin and G. Kats, "Greenhouse Warming: Comparative Analysis of Nuclear and Efficiency Abatement Strategies," Energy Policy, **16**(6), 538 (December 1988).

17. R. A. Krakowski, "Global Nuclear Energy/Materials Modeling in Support of Los Alamos Nuclear Vision Project: Long-Term Tradeoffs Between Nuclear- and Fossil-Fuel Burning," Global Foundation Energy Conference: Technology for the Global Economic, Environmental, and Survival and Prosperity, Miami Beach, FL (November 8-10, 1996), Plenum Press (to be published, 1997).

18. K. Hasselmann, S. Hasselmann, R. Giering, V. Ocana, and H. von Storch, "Optimization of CO_2 Emissions Using Coupled Integral Climate Response and Simplified Cost Models: A Sensitivity Study," N. Nakicenovic, W. D. Nordhaus, R. Richels, and F. L. Toth (Eds.), Proc. of Workshop on Climate Change: Integrating Science, Economics, and Policy, (March 19-20, 1996), International Institute for Applied Systems Analysis report CP-96-1 (December 1996).

19. J. Haraden, "An Improved Shadow Price for CO_2," Energy, **17**(5), 419 (1992).

20. C. Azar, "The Marginal Cost of CO_2 Emissions," Energy, **19**(2), 1255 (1994).

21. U. Cubasch, K. Hasselman, H. Hoeck, H. Maier-Riemer, E. Mikolajewicz, B. D. Santer, and R. Sausen, "Time-Dependent Greenhouse Warming Computations with a Coupled Ocean-Atmosphere Model," Climate Dynamics, **8**, 55 (1992).

22. K. Hasselmann, R. Sausen, E. Maier-Reimer, and R. Voss, "On the Cold Start Problem in Transient Simulations with Coupled Atmosphere-Ocean Models," Climate Dynamics, **9**, 53 (1993).

23. E. Maier-Reimer, "The Biological Pump in the Greenhouse," Global and Planetary Climate Change, **2**, 13 (1993).

24. E. Maier-Reimer and K. Hasselmann, "Transport and Storage of CO_2 in the Ocean: An Inorganic-Circulation Carbon Cycle Model, Climate Dynamics, **2**, 63 (1987).

25. S. Ghatak, Introduction to Development Economics, 3rd Ed., Routledge Press, London (1995)

26. P. Bagnoli, W. J. McKibbin, P. J. Wilcoxen, "Global Economics Prospects: Medium Term Projections and Structural Change," Brookings Discussion Paper No. 121 in International Economics (January 1996).

27. W. J. McKibbin and P. J. Wilcoxen, "The Theoretical and Empirical Structure of the G-Cubed Model," Brookings Discussion Paper No. 118 in International Economics (December 1995).

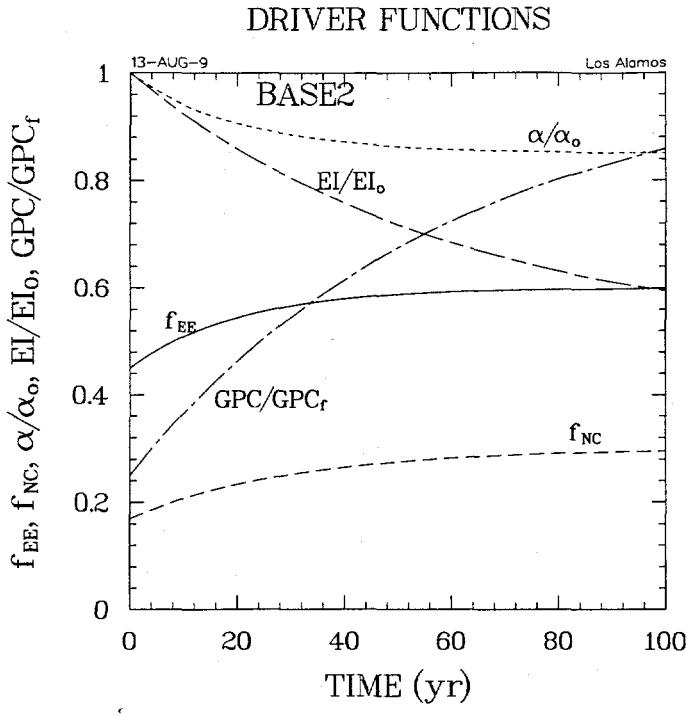

Figure 1. Driver functions used to evaluate base case (BASE2).

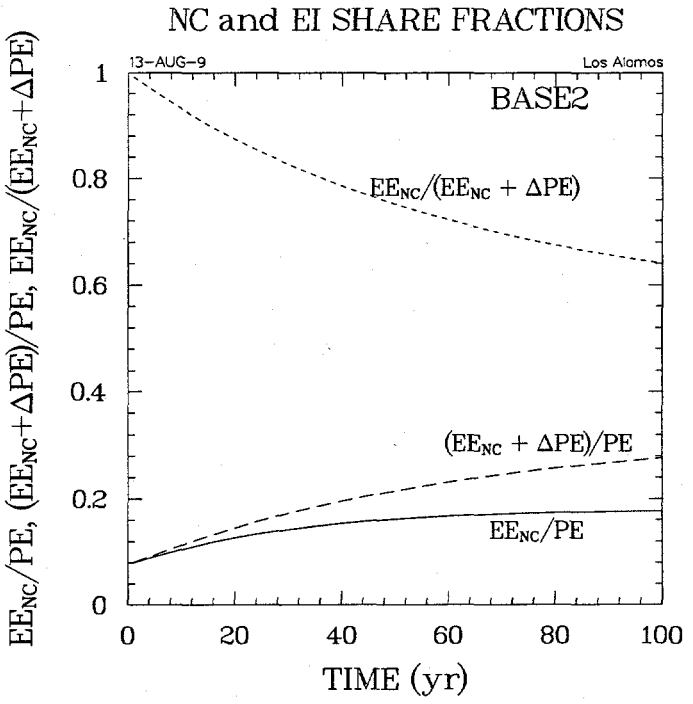

Figure 2. Relative fractions of Non-Carbon energy, EE_{NC}, and energy not used, ΔPE, as a function of time for the BASE2 driver functions (Fig. 1).

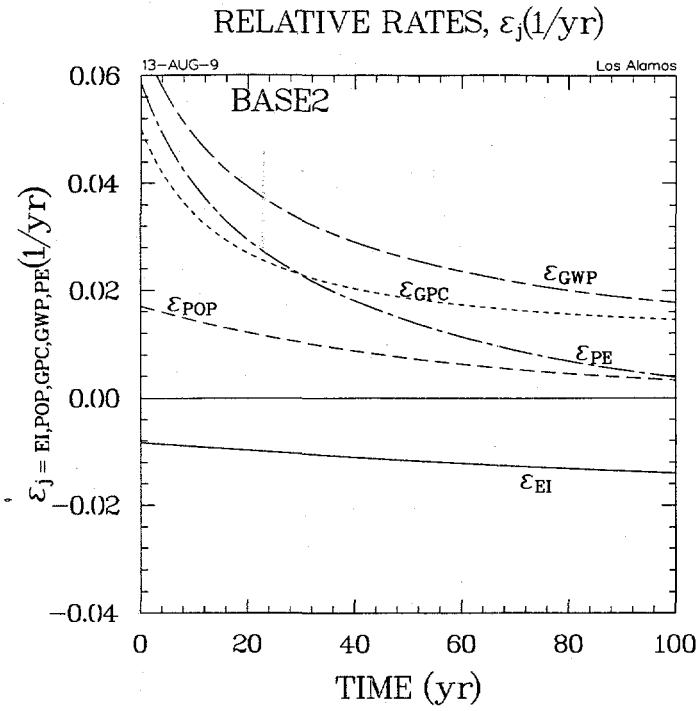

Figure 3. Relative rates resulting from base case (BASE2) driver functions.

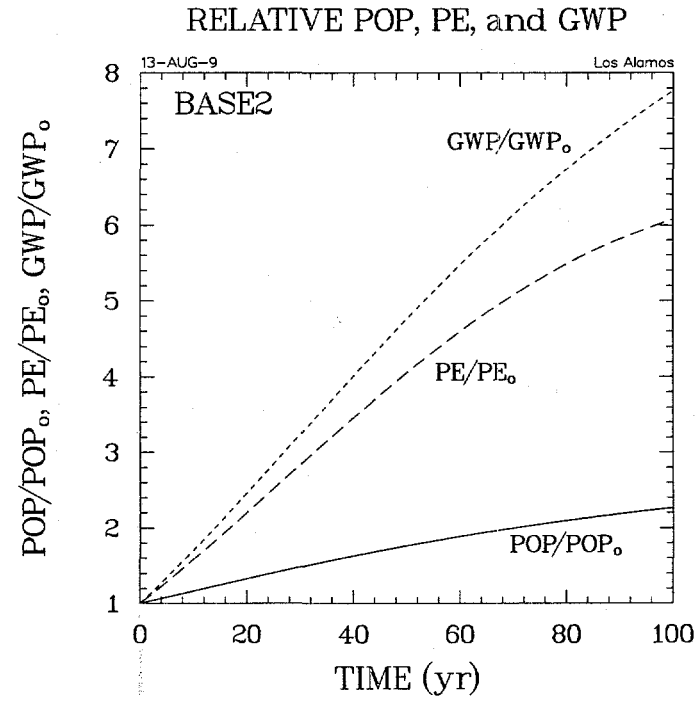

Figure 4. Relative population, primary energy, and GWP for the BASE2 driver functions (Fig. 1) and associated relative rates (Fig. 3).

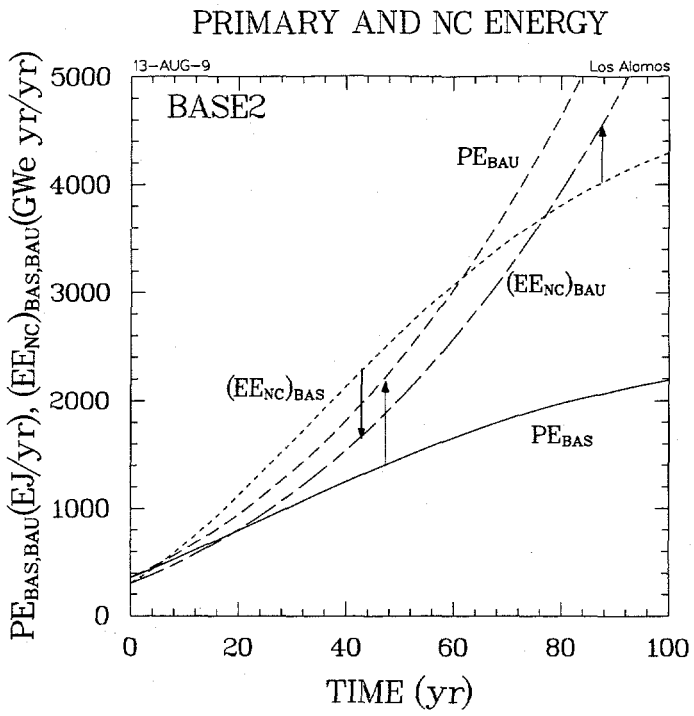

Figure 5. Primary and Non-Carbon (NC) energy for the BASE2 driver functions (Fig. 1) shown in comparison with the BAU case (Table I) values used to form benefit-to-cost ratios.

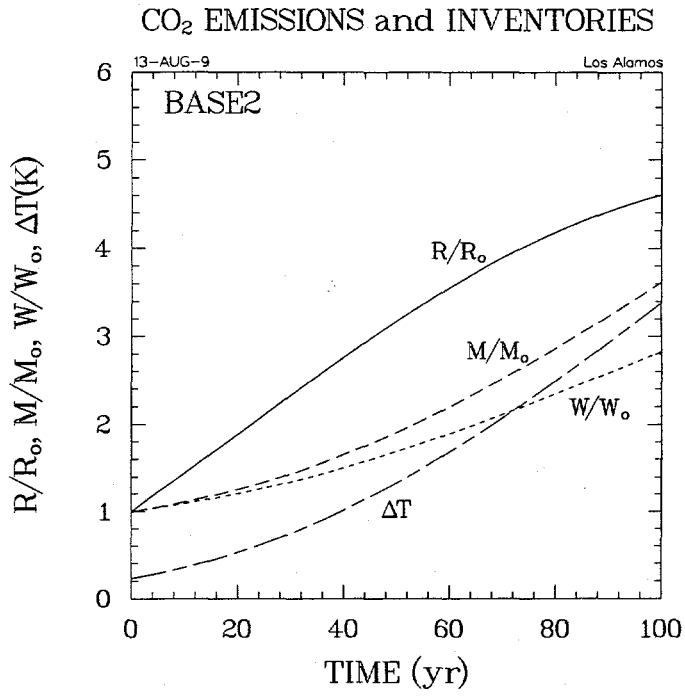

Figure 6. Relative emissions rated, R/R_o, integrated emissions, M/M_o, and, accumulations, W/W_o, of atmospheric carbon for the BASE2 conditions, as well as associated average global temperature rise.

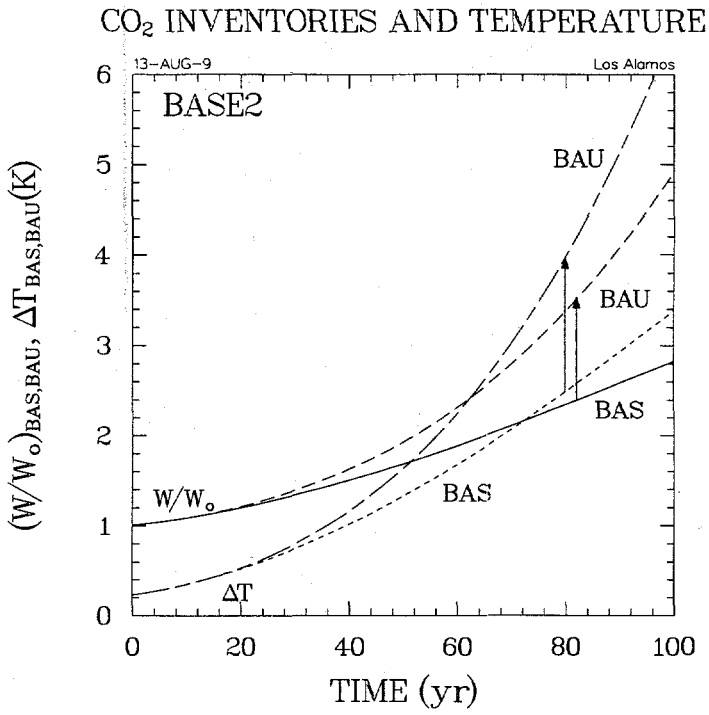

Figure 7. Relative accumulations, W/W_o, of atmospheric carbon and associated temperature rise for both BASE2 and BAU conditions.

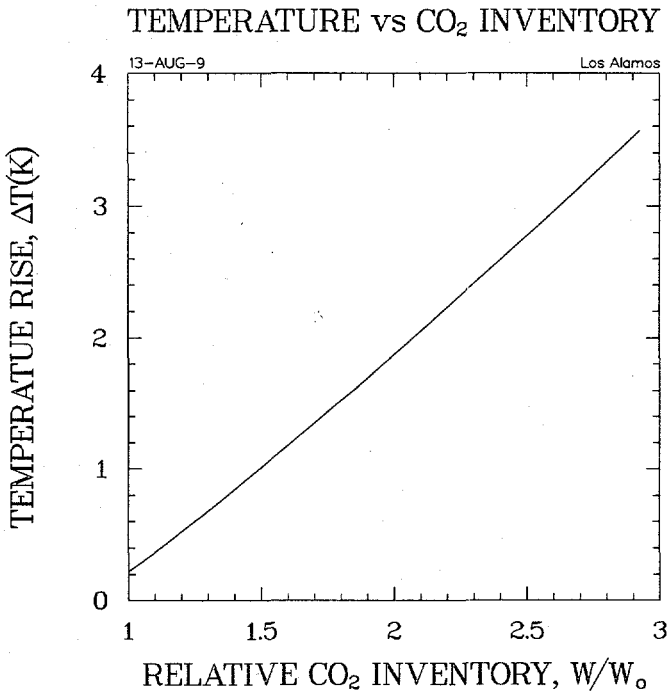

Figure 8. Relationship between instantaneous relative inventory of atmospheric CO_2 and average global surface temperature rise, as determined for BASE2 conditions using the integral response function reported in Ref. 18.

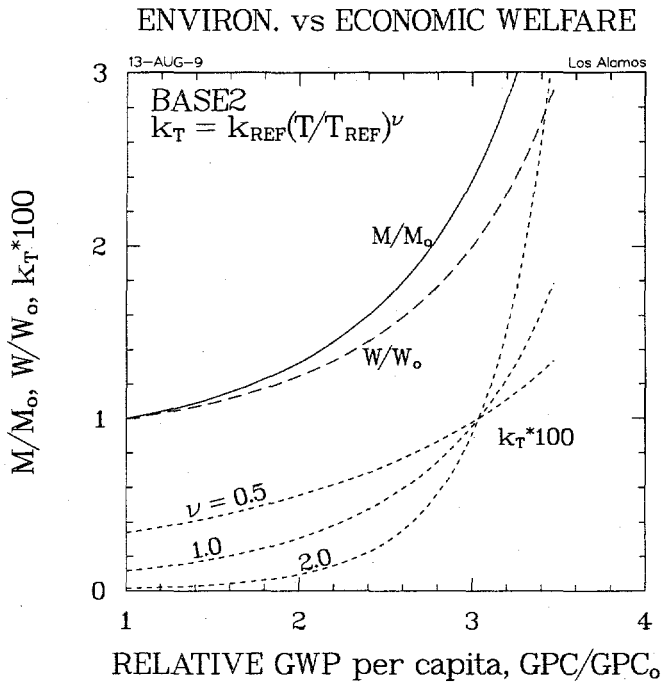

Figure 9. Relative integrated emissions and accumulations of atmospheric carbon *versus* relative improvement in human welfare for the BASE2 conditions, as well as related damage coefficient, k_T, for a range of temperature-rise exponent scalings [ν, Eq. (22)].

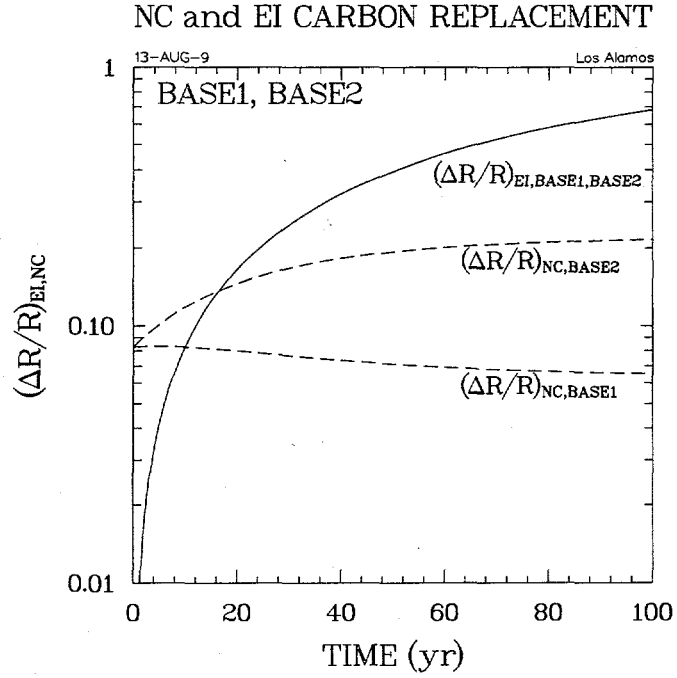

Figure 10. Relative carbon replacement for increased energy efficiency (*e.g.*, decreased EI) and increased NC electrical generation for the BASE2 conditions (Fig. 1 driver functions).

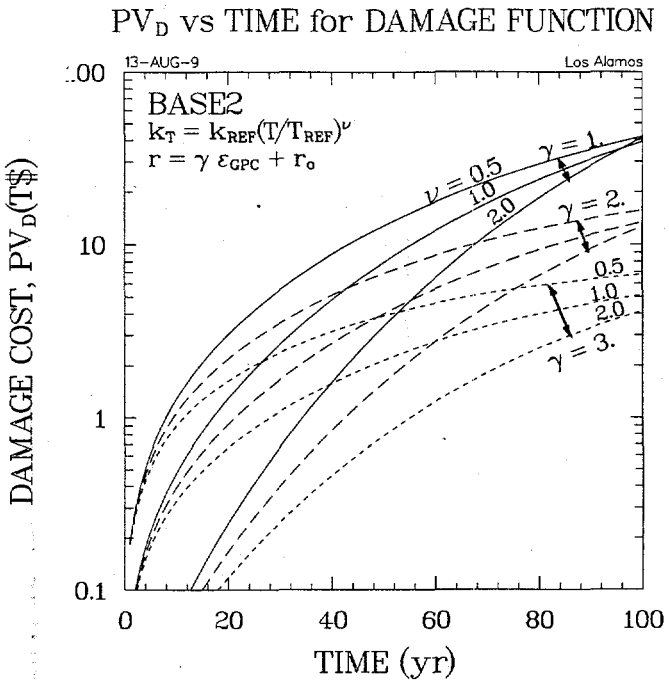

Figure 11. Time evolution of present value of damage costs, PV_D [Eq. (30)], evaluate directly from the damage function [Eqs. (22)-(24)] for a range of temperature-rise exponent scalings [ν, Eq. (22)] and EMUC [γ, Eq. (25)], for the BASE2 conditions.

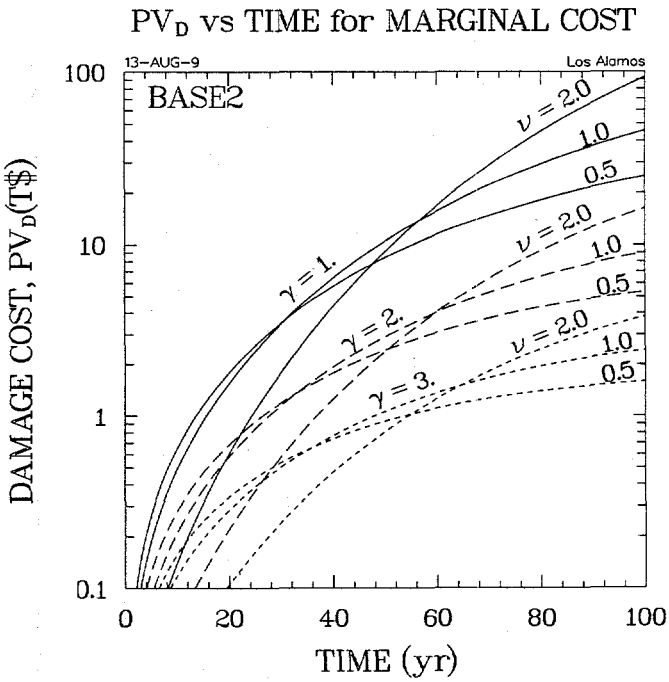

Figure 12. Time evolution of present value of damage costs, PV_D, evaluate from the marginal cost, UC_D [Eq. (24)] for a range of temperature-rise exponent scalings [ν, Eq. (22)] and EMUC [γ, Eq. (25)], for the BASE2 conditions.

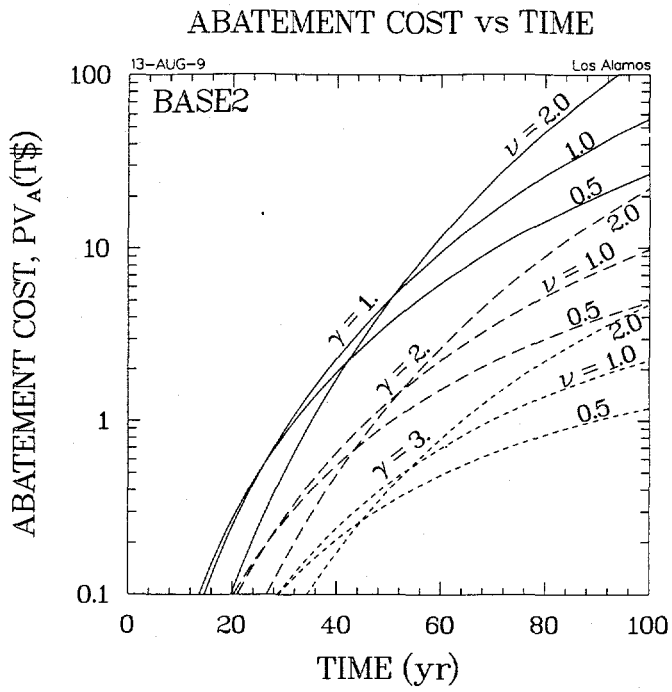

Figure 13. Time evolution of present value of abatement costs, PV_A [Eq. (29)], for a range of temperature-rise exponent scalings [ν, Eq. (22)] and EMUC [γ, Eq. (25)], for the BASE2 conditions.

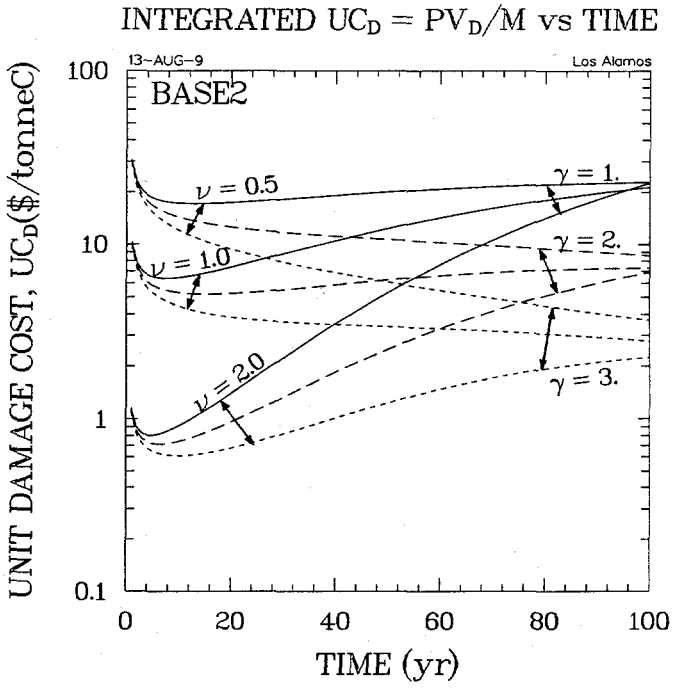

Figure 14. Integrated unit cost of damage, which is the ratio of the present value of damage cost base on marginal cost to the integrated atmospheric carbon emissions, for a range of temperature-rise exponent scalings [ν, Eq. (22)] and EMUC [γ, Eq. (25)], for the BASE2 conditions.

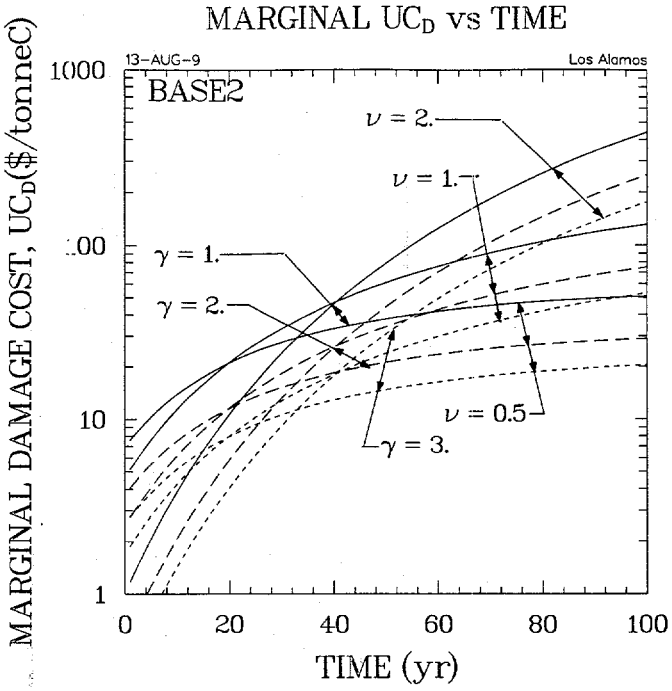

Figure 15. Time evolution of marginal unit cost of damage, UC_D [Eq. (24)], for a range of temperature-rise exponent scalings [ν, Eq. (22)] and EMUC [γ, Eq. (25)], for the BASE2 conditions.

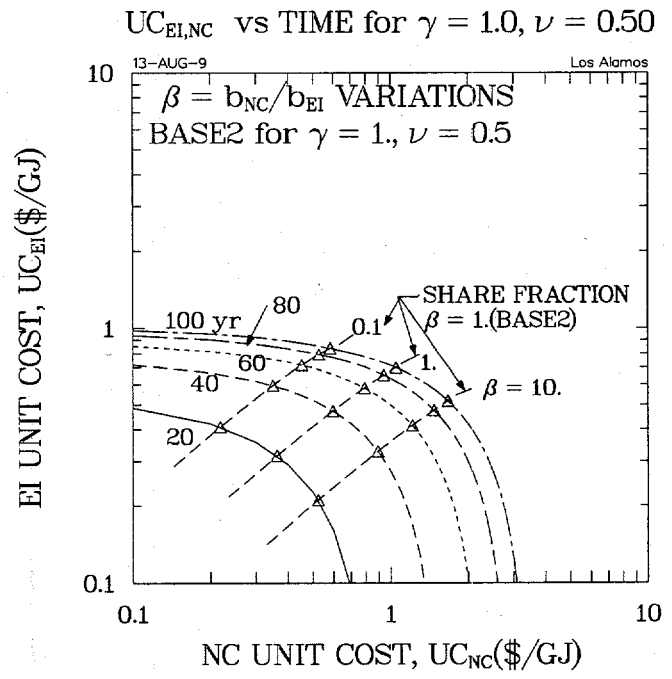

Figure 16A. Time evolution of indifference curves [Eq. (26)] for unit costs of abatement (*e.g.*, NC *versus* EI approaches) for EMUC γ = 1. and a range of temperature-rise exponent scalings for ν = 0.5, along with three values of NC *versus* EC weight ratios, $\beta = b_{NC}/b_{EI}$ [Eq. (27)].

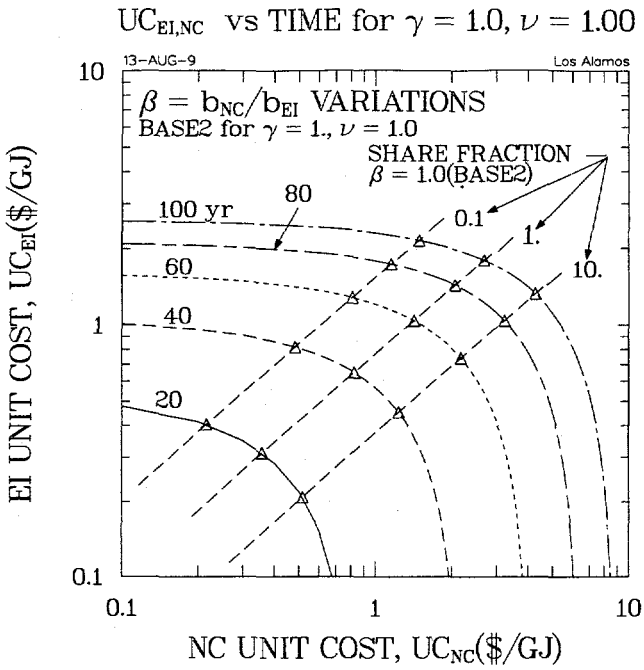

Figure 16B. Time evolution of indifference curves [Eq. (26)] for unit costs of abatement (*e.g.*, NC *versus* EI approaches) for EMUC γ = 1. and a range of temperature-rise exponent scalings for ν = 1.0, along with three values of NC *versus* EC weight ratios, $\beta = b_{NC}/b_{EI}$ [Eq. (27)].

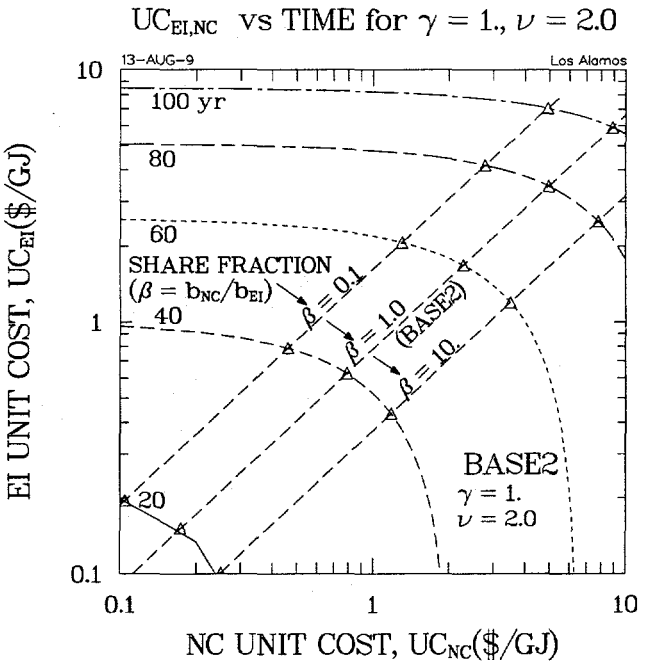

Figure 16C. Time evolution of indifference curves [Eq. (26)] for unit costs of abatement (*e.g.*, NC *versus* EI approaches) for EMUC γ = 1. and a range of temperature-rise exponent scalings for ν = 2.0, along with three values of NC *versus* EC weight ratios, $\beta = b_{NC}/b_{EI}$ [Eq. (27)].

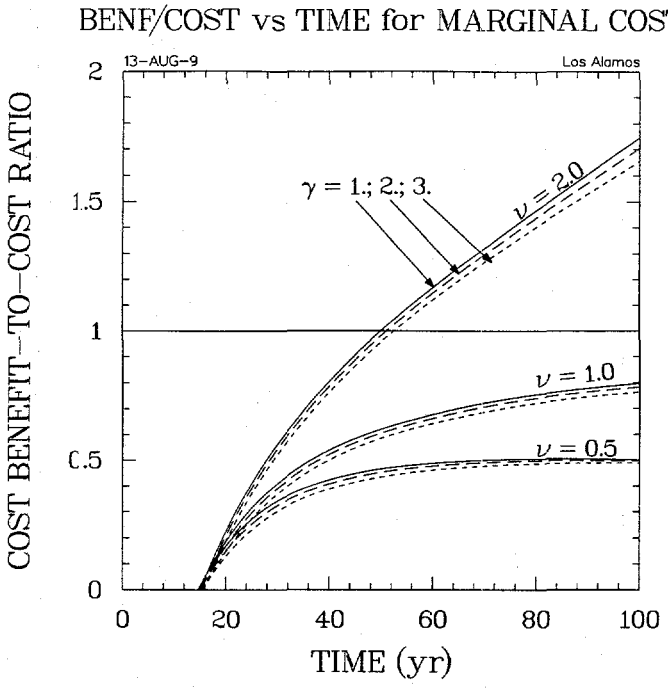

Figure 17. Time evolution of ratio of "benefits" (difference between BAU and BASE2 present value of damage costs) and "costs" (present value of abatement costs, Fig. 13) for range of temperature-rise scalings [ν, Eq. (22)] and EMUC [γ, Eq. (25)], for the BASE2 conditions.

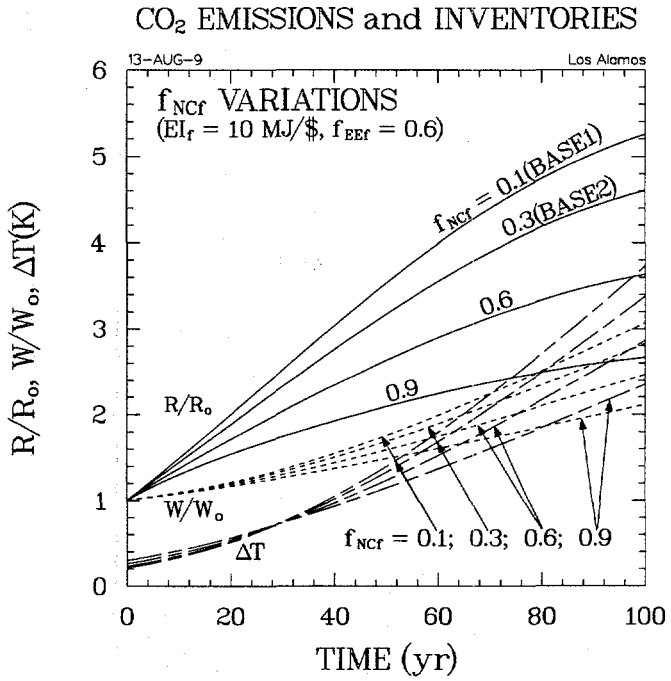

Figure 18. Impact of final NC implementation goal, f_{NCf}, on relative CO_2 emission rates, R/R_o, atmospheric accumulations, W/W_o, and temperature increases.

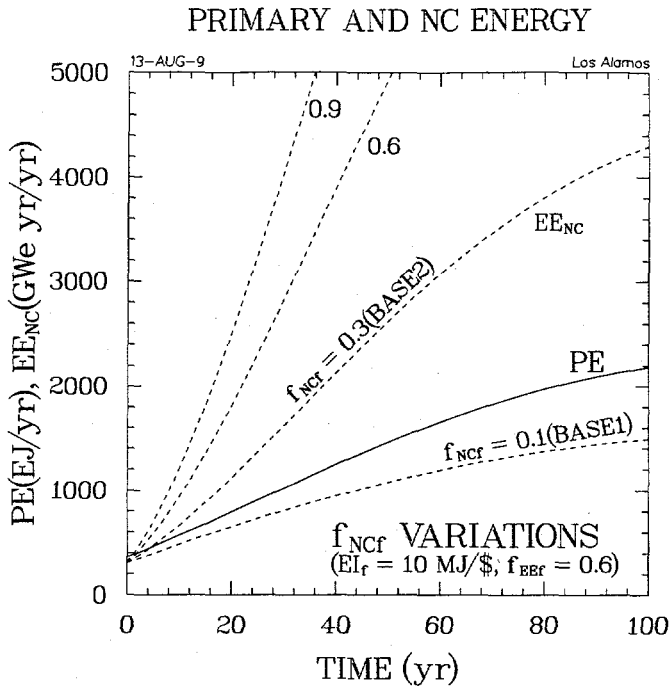

Figure 19. Impact of final NC implementation goal, f_{NCf}, on Non-Carbon electrical energy use, EE_{NC}.

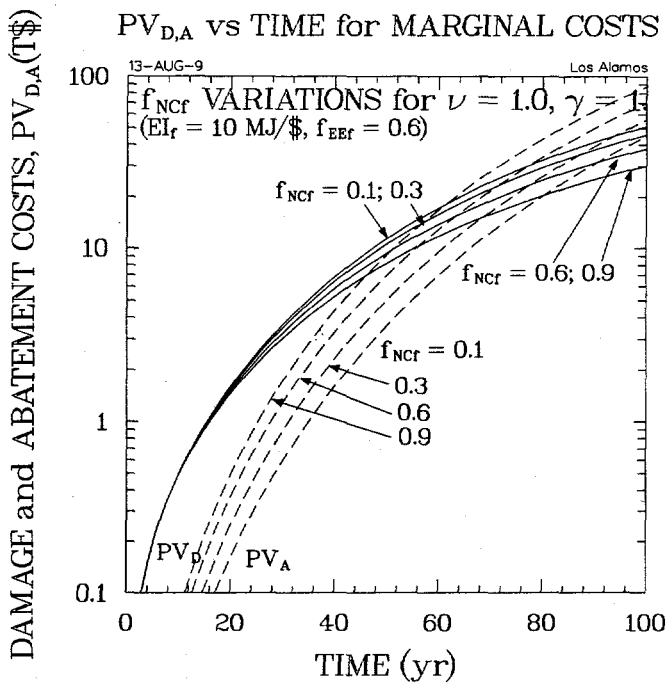

Figure 20. Impact of final NC implementation goal, f_{NCf}, on CO_2 damage and abatement costs for temperature-rise scalings exponent $\nu = 1$ and EMUC $\gamma = 1$.

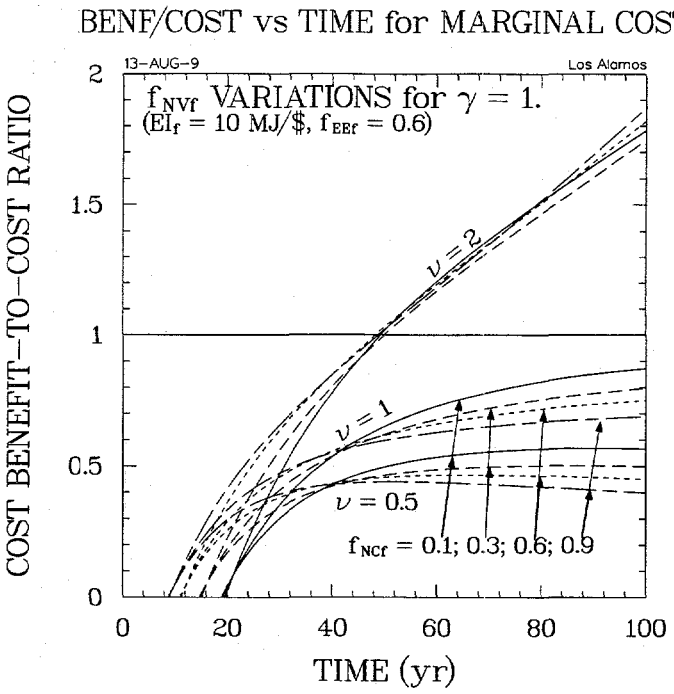

Figure 21. Impact of final NC implementation goal, f_{NCf}, on benefit-to-cost ratio for a range of temperature-rise scalings exponents [ν, Eq. (22)] and EMUC $\gamma = 1$.

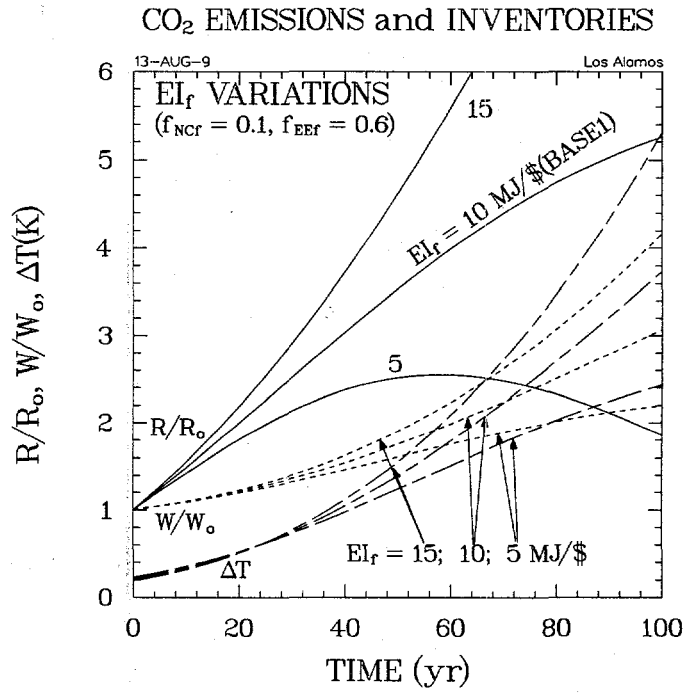

Figure 22. Impact of EI implementation goal, EI_f, on relative CO_2 emission rates, R/R_o, atmospheric accumulations, W/W_o, and temperature increases.

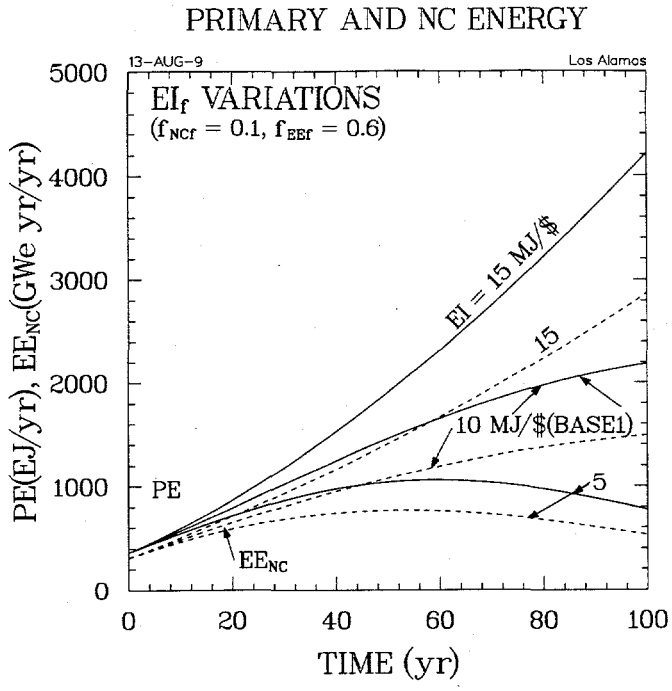

Figure 23. Impact of final EI implementation goal, EI_f, on total energy demand, PE, and Non-Carbon electrical energy use, EE_{NC}.

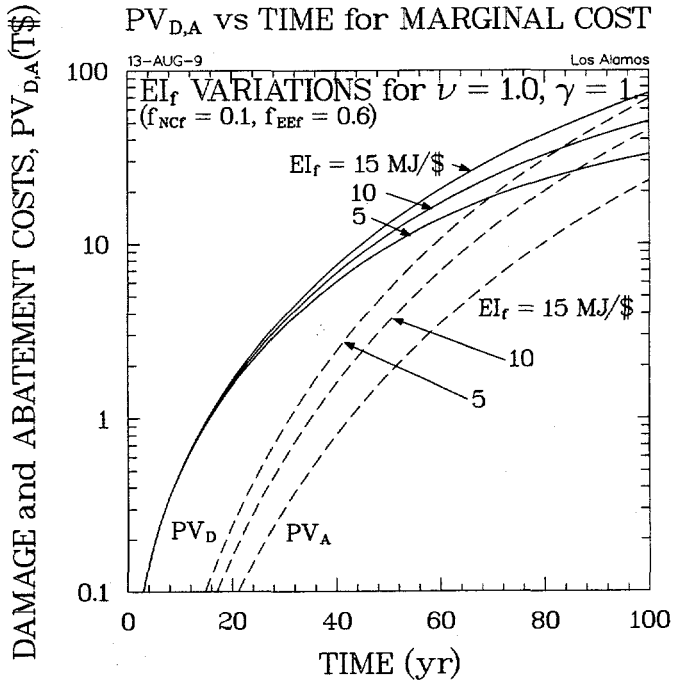

Figure 24. Impact of final EI implementation goal, EI_f, on CO_2 damage and abatement costs for temperature-rise scalings exponent $\nu = 1$ and EMUC $\gamma = 1$.

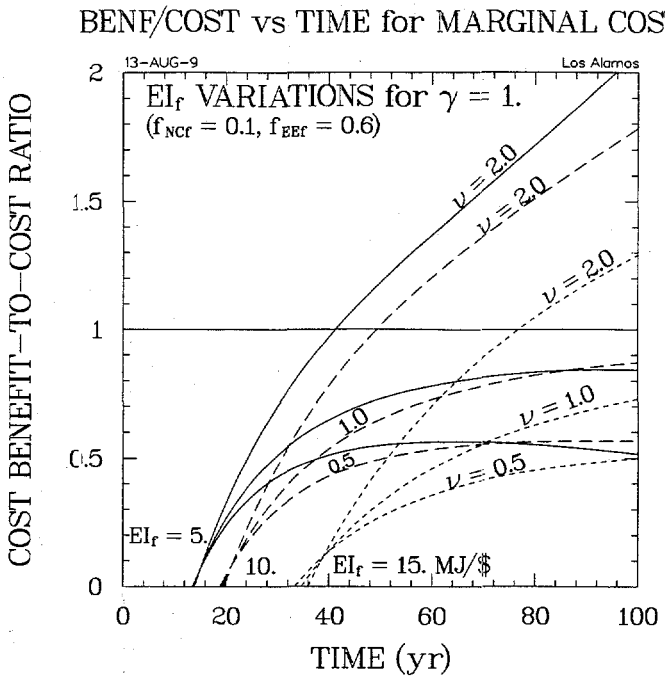

Figure 25. Impact of final EI implementation goal, EI_f, on benefit-to- cost ratio for a range of temperature-rise scalings exponents [ν, Eq. (22)] and EMUC ν = 1.

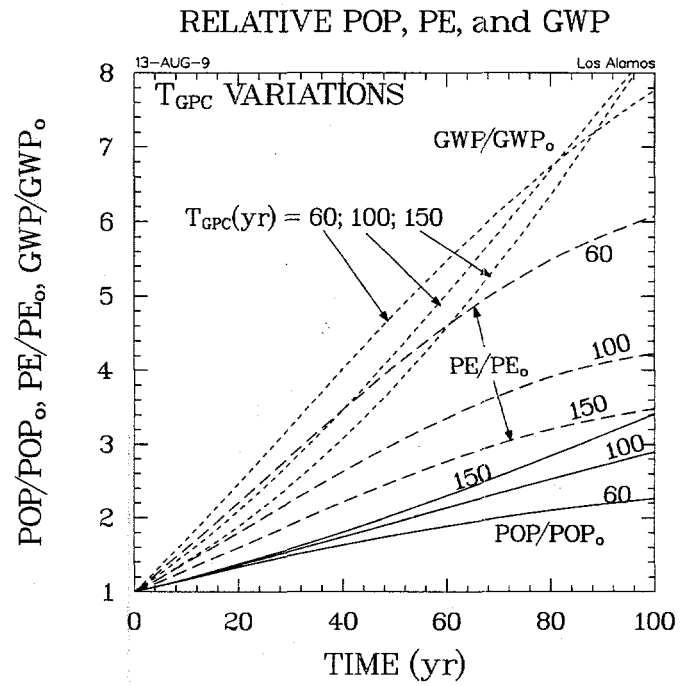

Figure 26. Impact of GWP *per-capita* growth rate on relative GWP, primary energy demand, PE/PE_o, and population, POP/POP_o.

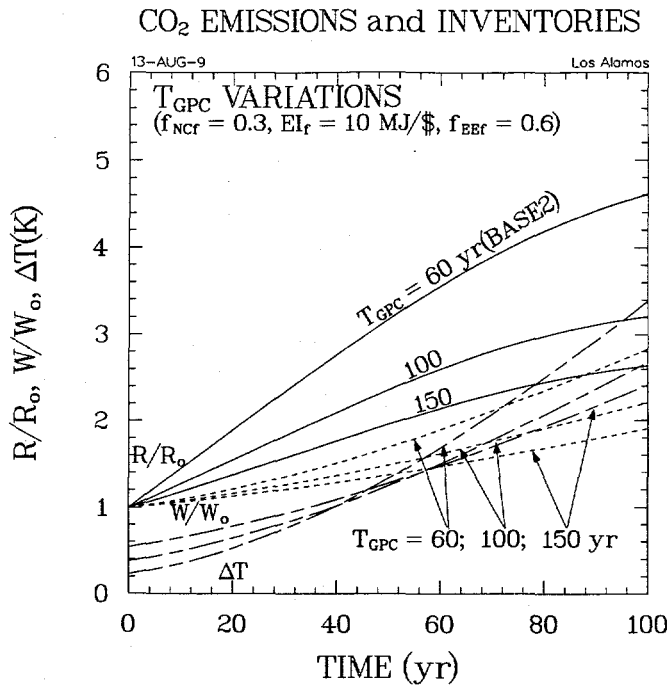

Figure 27. Impact of GWP *per-capita* growth rate on relative CO_2 emission rates, R/R_o, atmospheric accumulations, W/W_o, and temperature increases, for BASE2 conditions.

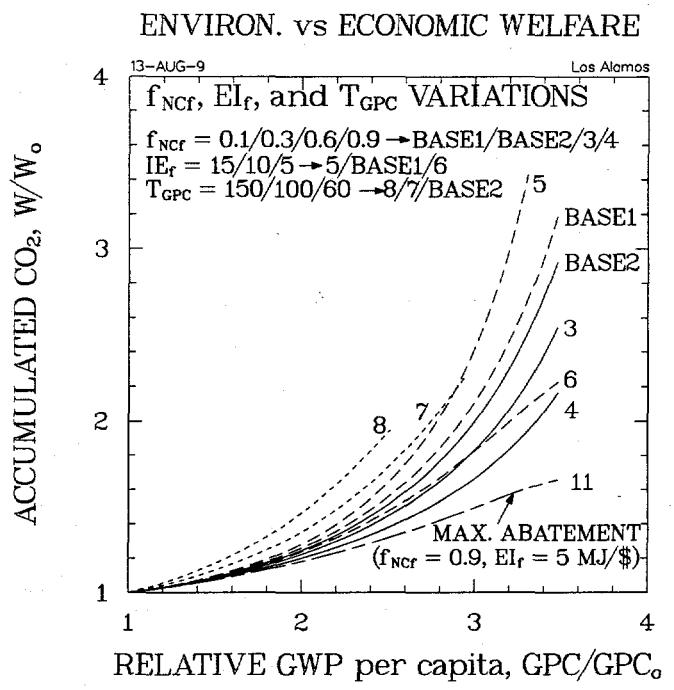

Figure 28. Impact of GWP *per-capita* growth rate on atmospheric carbon accumulations, W/W_o, *versus* relative improvement in human welfare; the impact in this W/W_o *versus* GWP/GWP_o "phase space" of the previously reported NC and EI final goal variations are also shown.

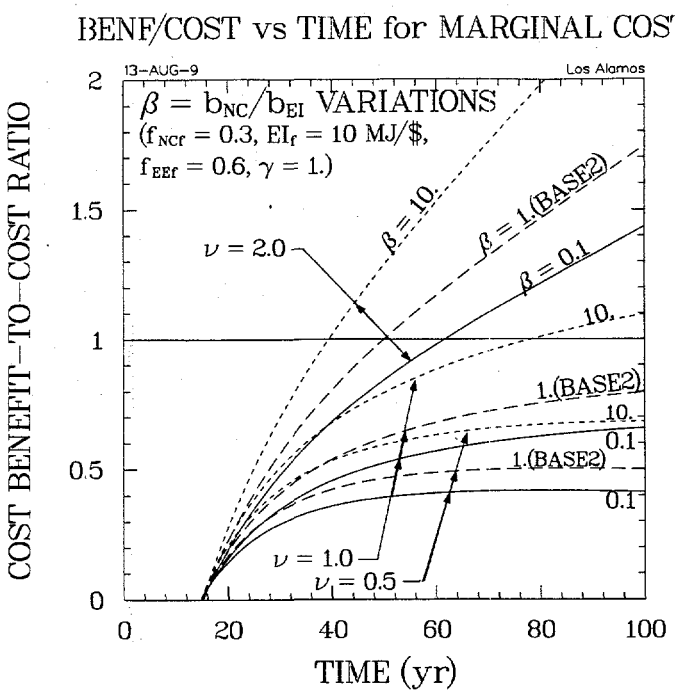

Figure 29. Impact of NC *versus* EI share fraction weights [Eq. (27), Fig. 16) on benefit-to-cost ratio for a range of temperature-rise scalings exponents [ν, Eq. (22)] and EMUC γ = 1., for BASE2 condition.

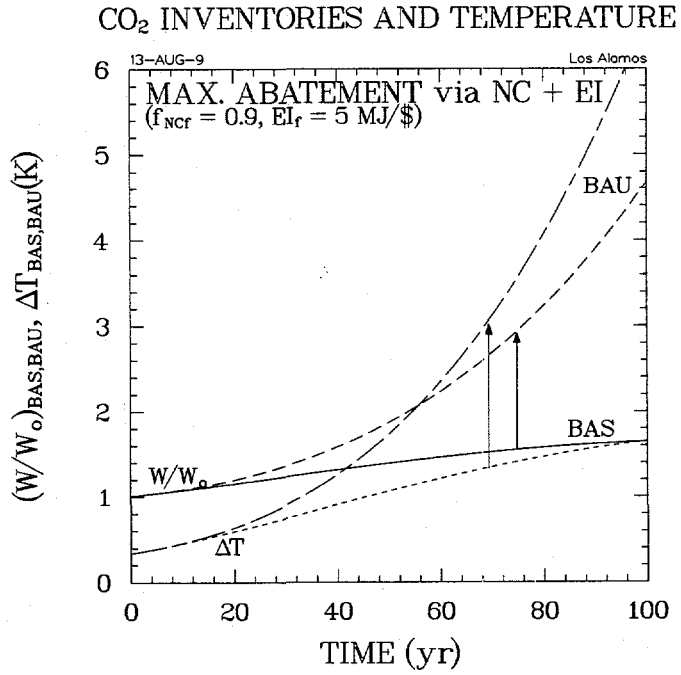

Figure 30. Relative accumulations, W/W_o, of atmospheric carbon and associated temperature rise for maximum use of NC and EI approaches to abatement and comparison with BAU conditions (refer to Fig. 8 for BASE2 conditions).

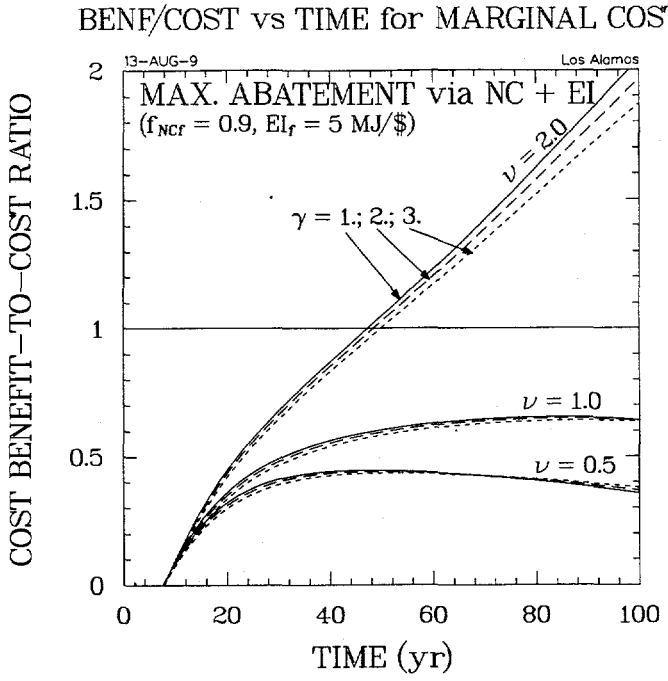

Figure 31. Time evolution of ratio of "benefits" (difference between BAU and base-case present value of damage costs) and "costs" (present value of abatement costs) for range of temperature-rise scalings [ν, Eq. (22)] and EMUC [γ, Eq. (25)], for the maximum use of NC and EI approaches to abatement and comparison with BAU conditions (refer to Fig. 17 for BASE2 conditions).

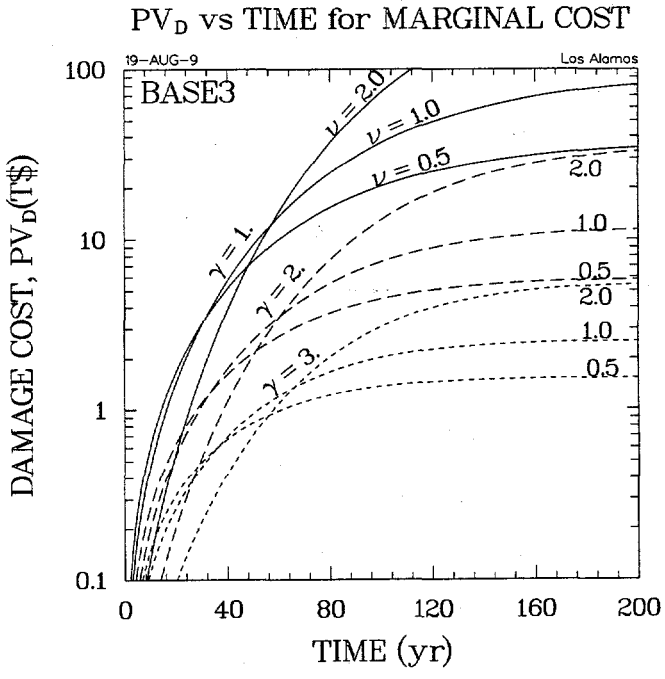

Figure 32. Time evolution of present value of damage costs, PV_D, evaluate from the marginal cost, UC_D [Eq. (24)] for a range of temperature-rise exponent scalings [ν, Eq. (22)] and EMUC [γ, Eq. (25)], for the BASE3 conditions.

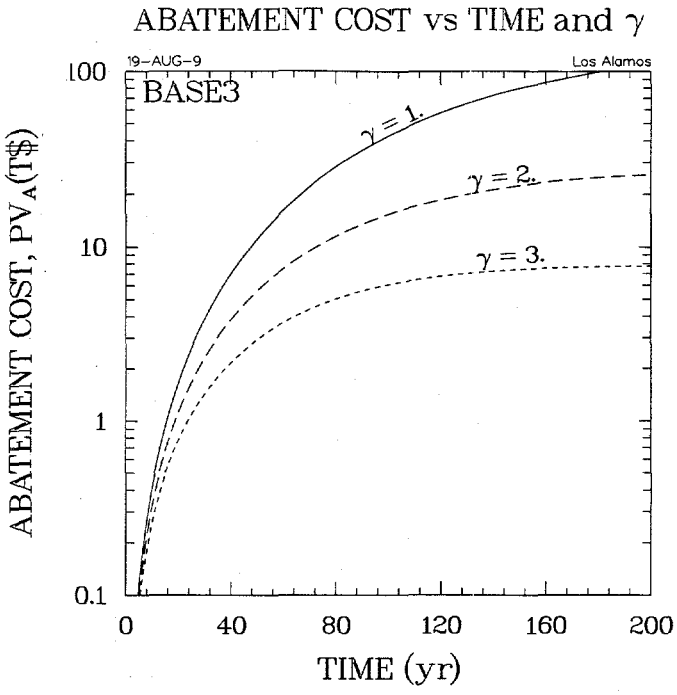

Figure 33. Time evolution of present value of abatement costs, PV_A [Eq. (29)], for a range of temperature-rise exponent scalings [ν, Eq. (22)] and EMUC [γ, Eq. (25)], for the BASE3 conditions.

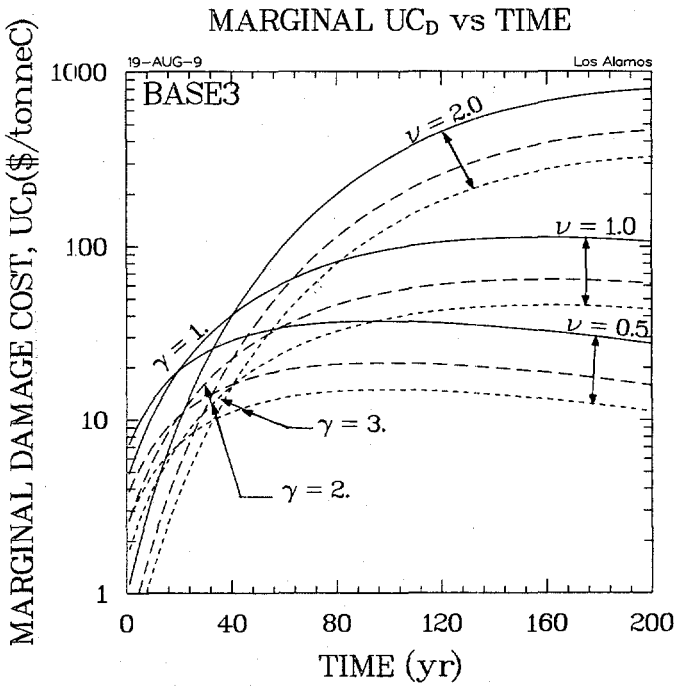

Figure 34. Time evolution of marginal unit cost of damage, UC_D [Eq. (24)], for a range of temperature-rise exponent scalings [ν, Eq. (22)] and EMUC [γ, Eq. (25)], for the BASE3 conditions.

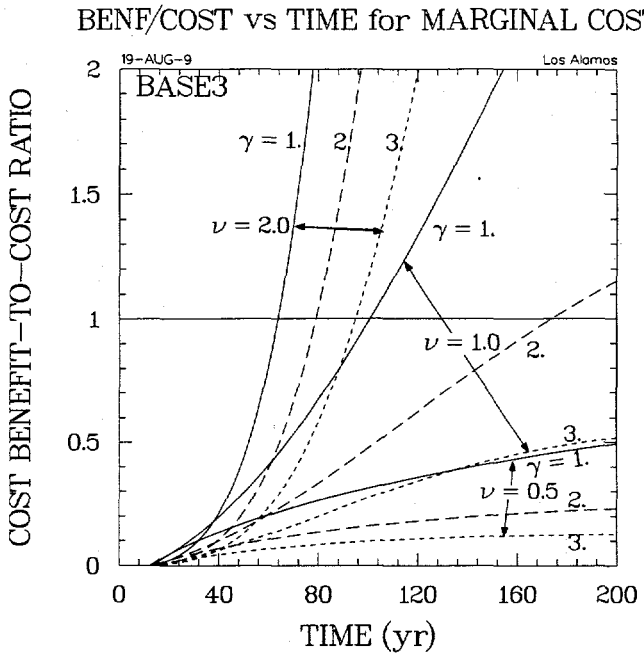

Figure 35. Time evolution of ratio of "benefits" (difference between BAU and BASE3 present value of damage costs) and "costs" (present value of abatement costs, Fig. 35) for range of temperature-rise scalings [ν, Eq. (22)] and EMUC [γ, Eq. (25)], for the BASE3 conditions.

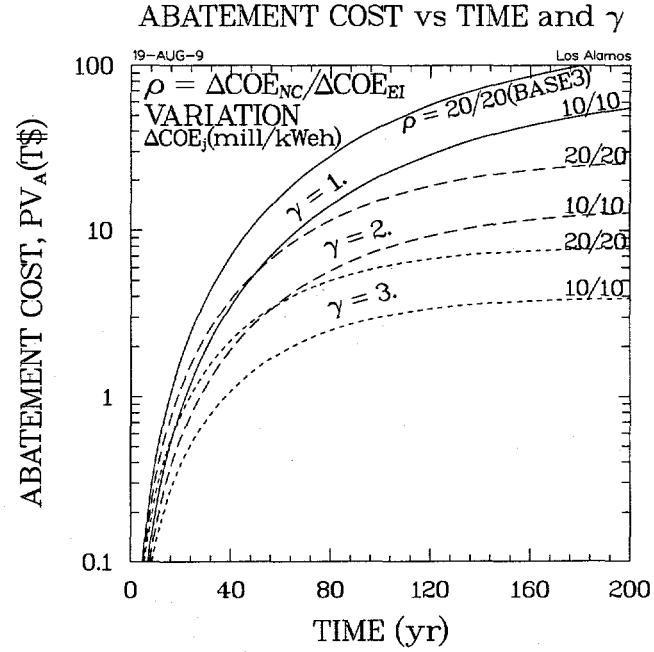

Figure 36. Time evolution of present value of abatement costs, PV_A [Eq. (29)], for a range of EMUC [γ, Eq. (25)] values and temperature-rise exponent scaling ν = 1.0 for high and low unit costs of NC and EI, ΔCOE_{NC} and ΔCOE_{EI}, respectively, for the BASE3 conditions.

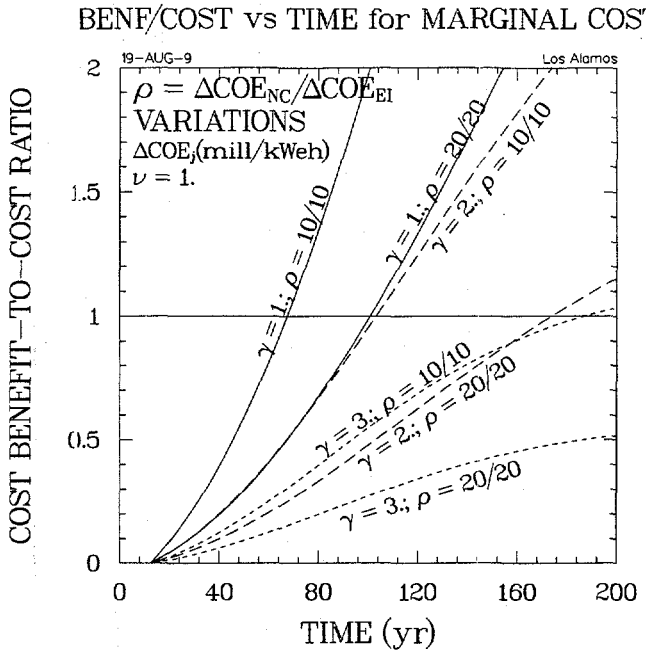

Figure 37. Time evolution of ratio of "benefits" (difference between BAU and BASE3 present value of damage costs) and "costs" (present value of abatement costs, Fig. 35) for a range of EMUC [γ, Eq. (25)] values and temperature-rise scaling ν = 1.0 for high and low unit costs of NC and EI, ΔCOE_{NC} and ΔCOE_{EI}, respectively, for the BASE3 conditions.

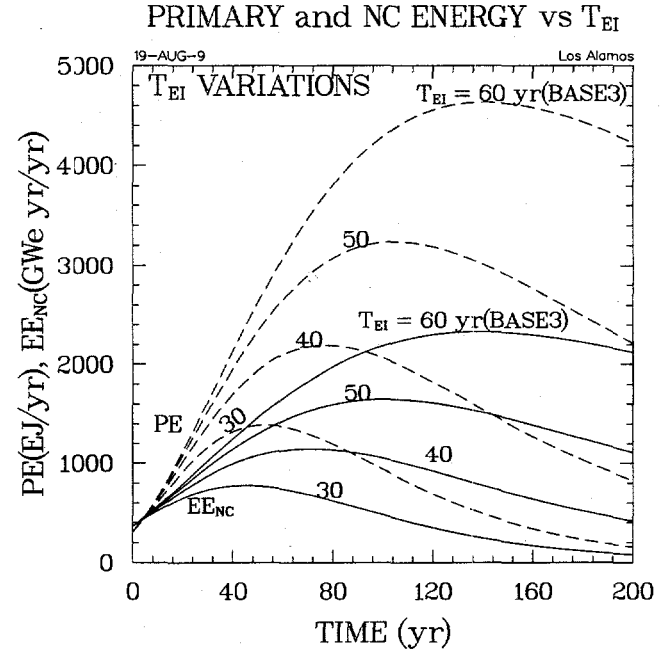

Figure 38. Time dependence of primary and NC electrical energy demand, PE and EE_{NC}, respectively, is the time scale for implementing decreases in energy intensity, T_{EI}(yr), is reduced from BASE2 conditions; all cases are referenced to a new base case, BASE3, which is BASE2 with increased time scale and $UC_{NC,EI}$ specified.

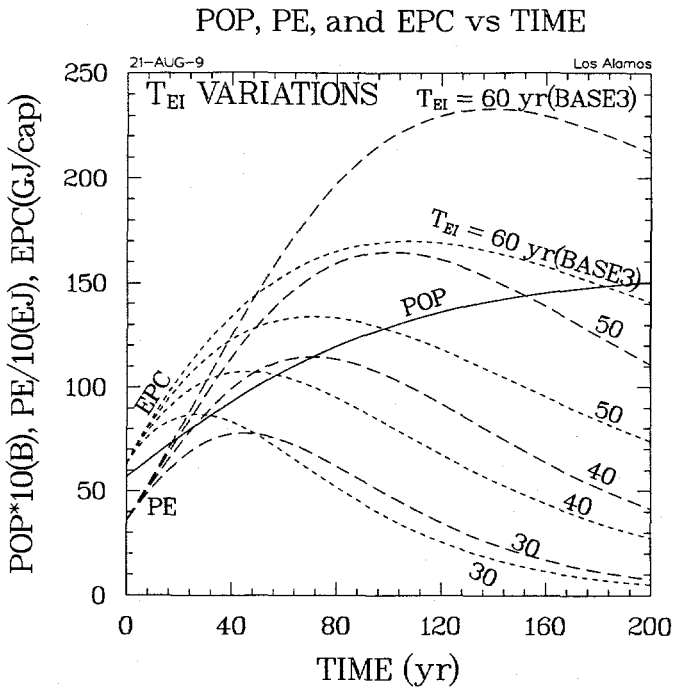

Figure 39. Comparison of primary energy and *per-capita* primary energy consumption *versus* time when T_{EI} is varied; based on EPC, values of T_{EI} below ~ 40 years are considered unrealistic.

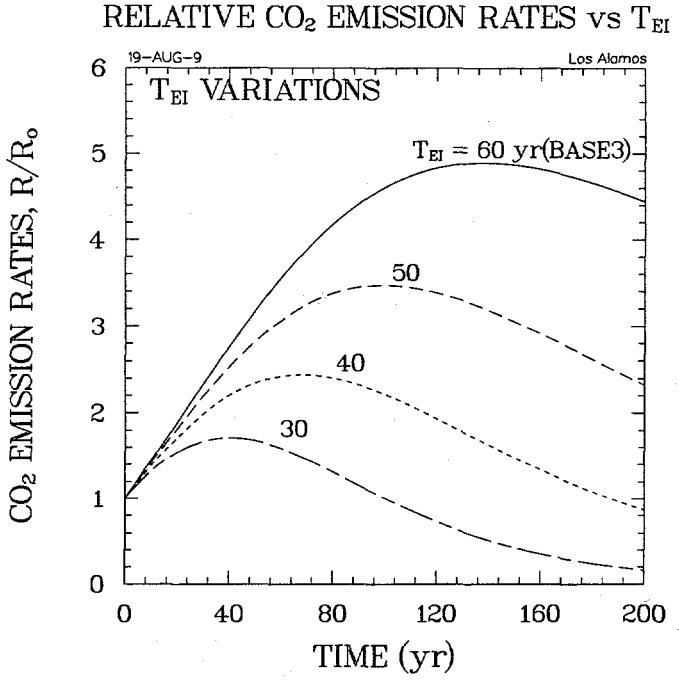

Figure 40A. Comparison of relative CO_2 emission rates, accumulations, and related temperature rises for T_{EI} variations about the BASE3 conditions (refer to Fig. 38 captions): Relative to CO_2 emission rates.

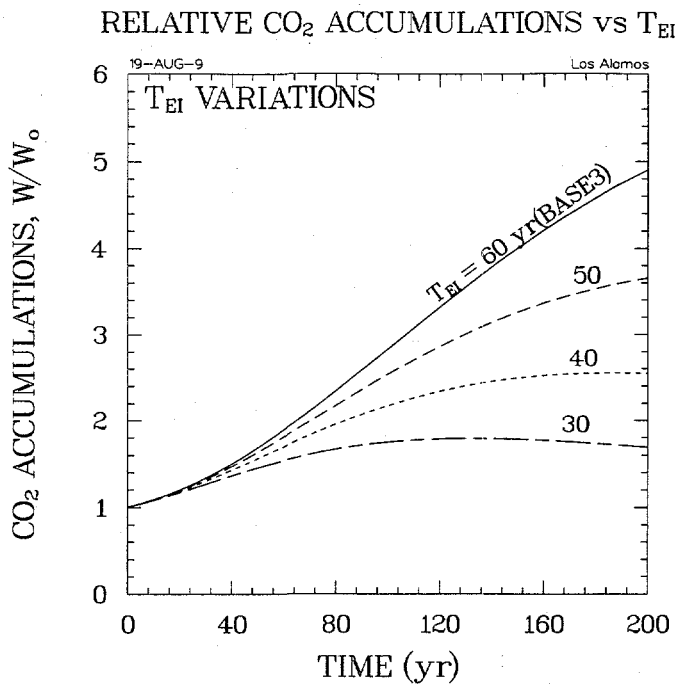

Figure 40B. Comparison of relative CO_2 emission rates, accumulations, and related temperature rises for T_{EI} variations about the BASE3 conditions (refer to Fig. 38 captions): Relative to CO_2 accumulations.

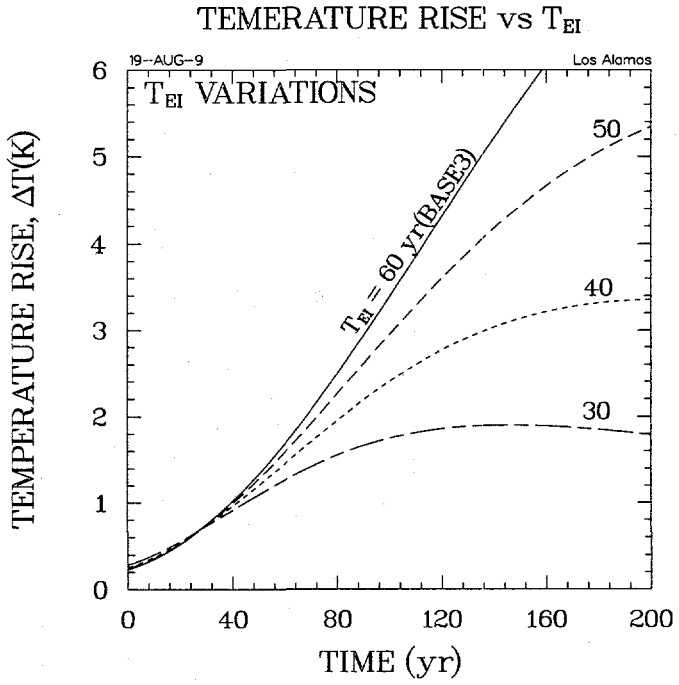

Figure 40C. Comparison of relative CO_2 emission rates, accumulations, and related temperature rises for T_{EI} variations about the BASE3 conditions (refer to Fig. 38 captions): Temperature rises.

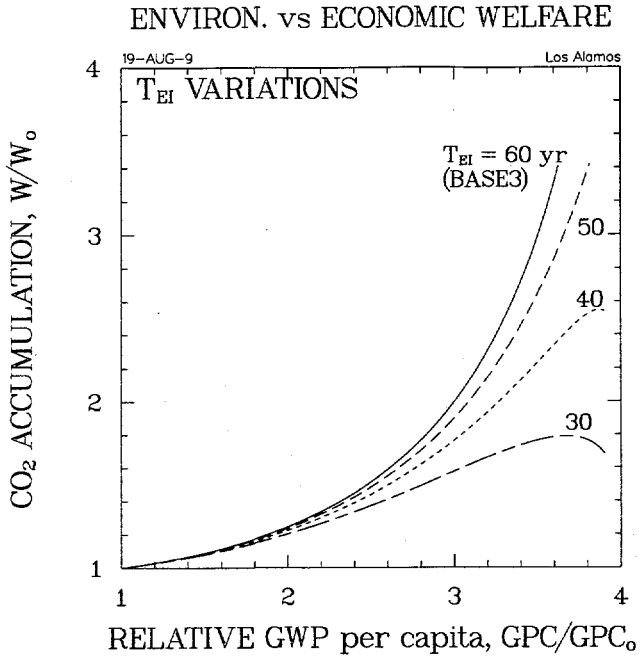

Figure 41. Impact of GWP *per-capita* growth rate on atmospheric carbon accumulations, W/W_0, *versus* relative improvement in human welfare; the impact in this W/W_0 *versus* GWP/GWP_0 "phase space" of the time scale for EI decrease, T_{EI}, is shown relative to BASE3 conditions.

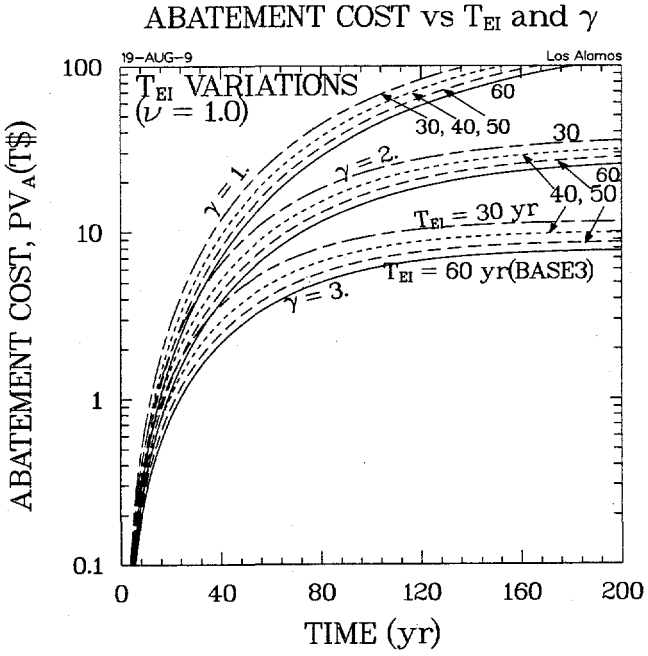

Figure 42. Time evolution of present value of abatement costs, PV_A [Eq. (29)], for a range of EMUC [γ, Eq. (25)] values and temperature-rise exponent scaling ν = 1.0 for a range of time scales assumed for the implementation of decreased EI relative to the BASE3 conditions.

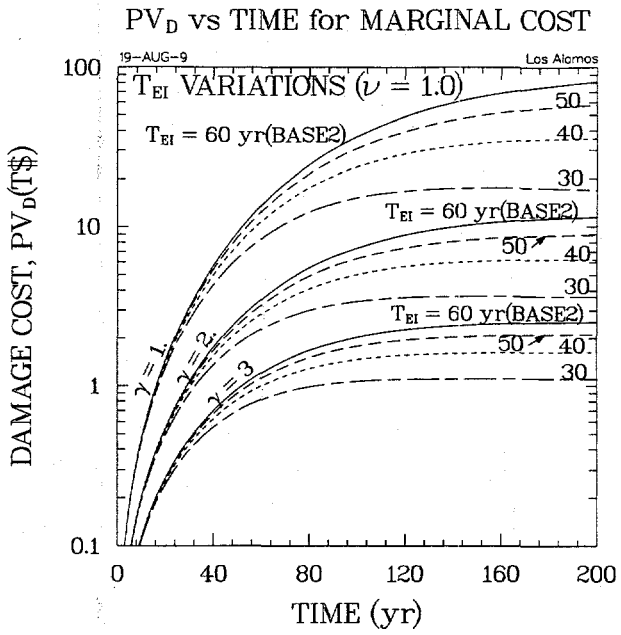

Figure 43. Time evolution of present value of damage costs, PV_D, evaluate from the marginal cost, UC_D [Eq. (24)], for a range of EMUC [γ, Eq. (25)] values and a temperature-rise exponent scaling [Eq. (22)] ν = 1.0 for a range of time scales assumed for the implementation of decreased EI relative to the BASE3 conditions.

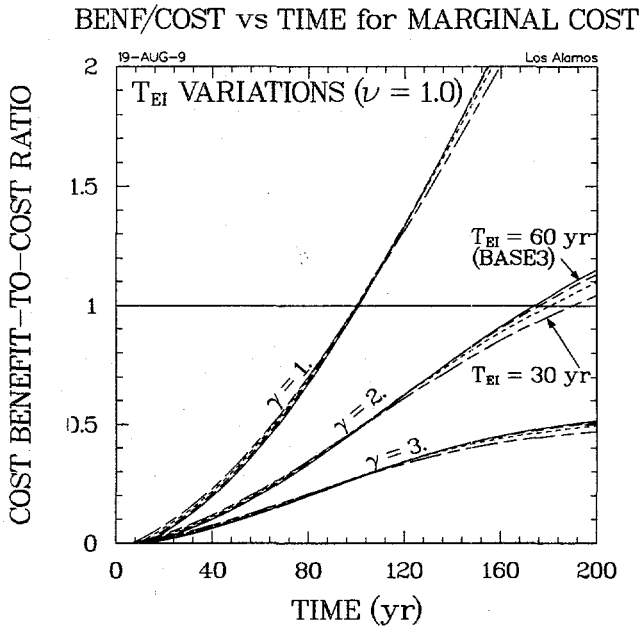

Figure 44. Time evolution of ratio of "benefits" (difference between BAU and BASE3 present value of damage costs) and "costs" (present value of abatement costs, Fig. 43) for a range of EMUC [γ, Eq. (25)] values and temperature-rise scaling ν = 1.0 for for a range of time scales assumed for the implementation of decreased EI relative to the BASE3 conditions.

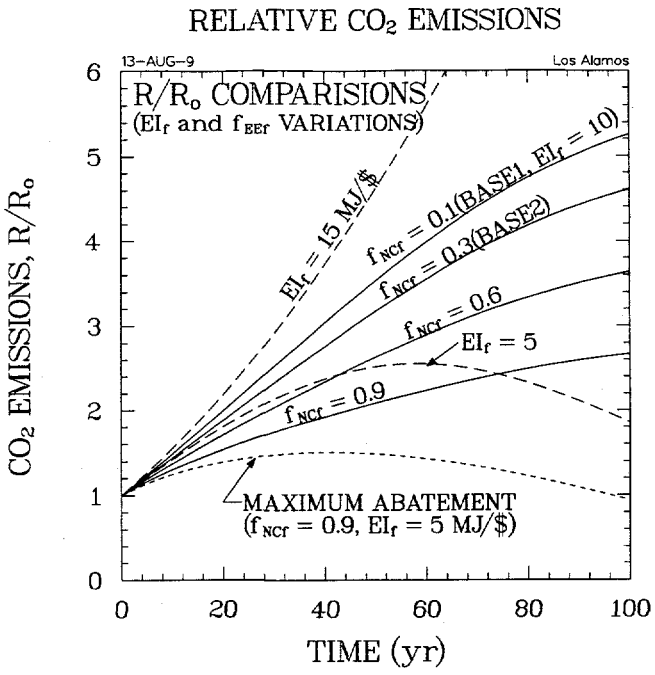

Figure 45A. Comparison of relative CO_2 emission rates, accumulations, and related temperature rises for NC and EI variations, as well as for the "maximum abatement" case (f_{NCf} = 0.9, EI_f = 5 MJ/$): Relative CO_2 emission rates.

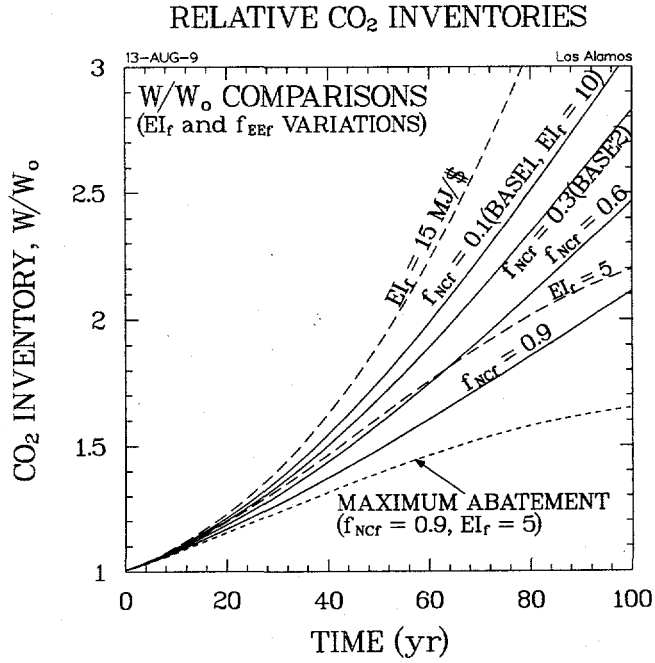

Figure 45B. Comparison of relative CO_2 emission rates, accumulations, and related temperature rises for NC and EI variations, as well as for the "maximum abatement" case (f_{NCf} = 0.9, EI_f = 5 MJ/$): Relative CO_2 accumulations.

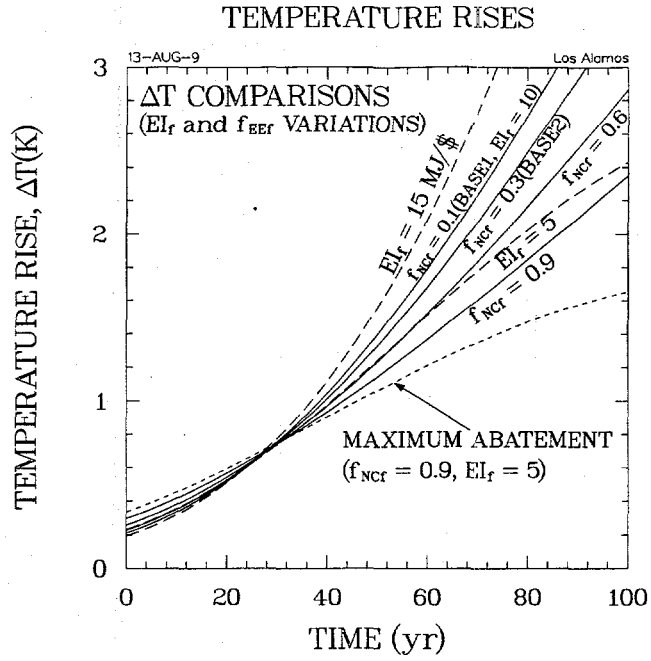

Figure 45C. Comparison of relative CO_2 emission rates, accumulations, and related temperature rises for NC and EI variations, as well as for the "maximum abatement" case ($f_{NCf} = 0.9$, $EI_f = 5$ MJ/\$): Temperature rises.

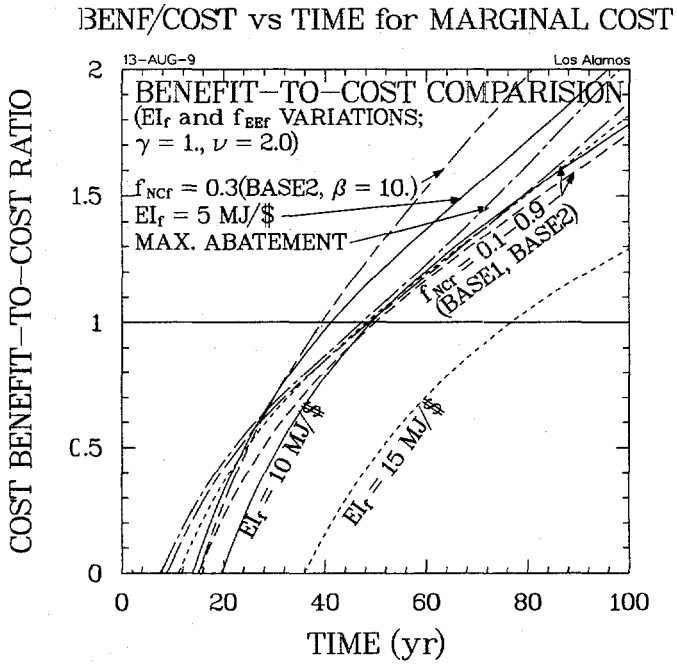

Figure 46. Comparison of benefit-to-cost ratios for NC and EI variations, as well assure the "maximum abatement" case ($f_{NCf} = 0.9$, $EI_f = 5$ MJ/\$) and the $\beta = b_{NC}/b_{EI} = 10$ case.

Table I. Fixed Input Parameters[a]

initial carbon emission rate, R_o(GtonneC/yr)	6.0
initial atmospheric carbon inventory, M_o(Gtonne)	740.
initial primary energy use, PE_o(EJ/yr)	360.
initial population, POP_o(B)	5.7
initial carbon emission coefficient, α_o(Mtonne/EJ)	18.1
final carbon emission coefficient, α_f(Mtonne/EJ)	15.3
carbon emission coefficient time, T_α(yr)	20.
carbon emission coefficient initial rate, $\varepsilon_{\alpha o}$(1/yr)	-0.0075
initial electric energy fraction, f_{EEo}	0.45
final electric energy fraction, f_{EEf}	0.60
electric energy time, T_{EE}(yr)	20.
electric energy fraction initial rate, ε_{fEEo}(1/yr)	0.0167
initial NC electric energy fraction, f_{NCo}	0.17
final NC electric energy fraction, f_{NCf}[b]	0.1-0.9
NC electric energy fraction time, T_{NC}(yr)	30.
NC electric energy fraction initial rate, ε_{fNCo}(1/yr)	-0.0137
initial energy intensity, EI_o(MJ/$)	20.0
final energy intensity, EI_f(MJ/$)[b]	5.-15.
energy intensity time, T_{EI}(yr)	60.
initial energy intensity rate, ε_{EIio}(1/yr)	-0.0083
initial GNP *per capita*, GPC_o($/*capita*)	5000.
final GNP *per capita*, GPC_f($/*capita*)	20000.
GNP *per capita* time, T_{GPC}(yr)[b]	60.-150.
initial GNP *per capita* time constant, ε_{GPCo}(1/yr)	0.0500
initial population growth rate, ε_{POPo}(1/yr)	0.0170
final population growth rate, ε_{POPf}(1/yr)	0.0020
nominal thermal-electric conversion efficiency, η_{TH}	0.35
carbon displacement costs:	
• EI carbon displacement cost, ΔCOE_{EI}(mill/kWeh)[b,c]	10. - 2.0
• EI carbon displacement unit cost, UC_{EIo}($/tonneC)[b,c]	1.0 - 2.0
• NC carbon displacement cost, ΔCOE_{NC}(mill/kWeh)[b,c]	10.
• NC carbon displacement unit cost, UC_{NCo}($/tonneC)[b,c]	54.
logit share parameters:	
• EI logit exponent, r_{EI}	3.0
• NC logit exponent, r_{NC}	3.0
• EI logit weight, b_{EI}	1.0
• NC logit weight, b_{NC}	1.0
BAU case parameters	
• final carbon emission coefficient, α_f^{BAU} (Mtonne/EJ)	15.3

• initial carbon emission coefficient rate, eps_{α}^{BAU} (1/yr)	-0.0075
• final electric energy fraction, f_{EEf}^{BAU}	0.45
• initial electrical energy fraction rate, eps_{EEf}^{BAU} (1/yr)	0.0
• final NC energy fraction, f_{NCf}^{BAU}	0.17
• initial NC energy fraction rate, eps_{NCf}^{BAU} (1/yr)	0.0
• final energy intensity, EI_{f}^{BAU} (MJ/$)	20.0
• initial energy intensity rate, eps_{EI}^{BAU} (1/yr)	0.0
parameters for CO_2 model[d]	
• start of industrial era, t_o	1800
• reference year, t_1	1995
• CO_2 atmospheric inventory in year t_o, W_o(GtonneC)	594.
• pre-1995 CO_2 growth time, τ_{CO_2} (yr)[e]	23.2
• interconnect time	1994-95
• CO_2 inventory at connection time, W_1(Gtonne)	702.
• elasticity of marginal utility of consumption, γ[b]	1.-3.
• damage function exponent, ν[b]	0.5-2.0
• reference damage per gnp, k_{REF}	0.01
• reference temperature rise for k_{REF}, T_{REF}(K)	2.0
• pure time preference, r_o(1/yr)	0.0

(a) Please refer to Nomenclature for definition of notation.

(b) Subject to parameter variation in this study; refer to Table III.

(c) Most cases reported used $UC'_{EI,NC}$($/GJ) values derived from the indifference relationship [Eq. (26)], and the assumed share fraction [Eq. (27)].

(d) Using model reported in Ref.-18 and fitting parameters listed in Table II.

(e) Equation (21), BASE2 conditions.

Table II. Summary of Amplitudes and Time Constants Used to Fit Integral Response Functions to CGCM Results[18]

Index	Inventory Response, W(Gtonne) R_W [Eq. (14)]		Temperature Response, ΔT(K) R_T^* [Eq. (15)]	
j	A_j^W	t_j^W	A_j^T	t_j^T
0	0.070	∞	0.0	---
1	0.648	258.5	0.8	2.9
2	0.101	71.9	0.3	40.
3	0.097	71.6	1.4	300.
4	0.084	1.6	---	---

Table III. Summary of Parameter Variation Logic

Case	NC Final Fraction f_{NCf}	Final Energy Intensity EI_f (MJ/$)	GPC Growth Time T_{GPC} (yr)	NC *versus* EI Preference Weights b_{NC}/b_{EI}	NC and EI Unit Cost Mode[c] UC_{NC} (mill/kWeh)	UC_{EI} (mill/kWeh)	EI (MJ/$) Reduction Time T_{EI} (yr)
1[a]	0.1	10.	60.	1.0	---		60.
2[b]	0.3	10.	60.	1.0	---		60.
3	0.6	10.	60.	1.0	---		60.
4	0.9	10.	60.	1.0	---		60.
5	0.1	15.	60.	1.0	---		60.
6	0.6	5.	60.	1.0	---		60.
7	0.3	10.	100.	1.0	---		60.
8	0.3	10.	150.	1.0	---		60.
9	0.3	10.	60.	0.1	---		60.
10	0.3	10.	60.	10.0	---		60.
11	0.9	5.	60.	1.0	---		60.
12	0.3	10.	60.	1.0	10.	10.	60.
13	0.3	10.	60.	1.0	10.	20.	60.
14	0.3	10.	60.	1.0	20.	10.	60.
15[d]	0.3	10.	60.	1.0	20.	20.	60.
16	0.3	10.	60.	1.0	10.	10.	50.
17	0.3	10.	60.	1.0	10.	20.	40.
18	0.3	10.	60.	1.0	20.	10.	30.

(a) Basecase 1 (BASE1)
(b) Basecase 2 (BASE2)
(c) For no value indicated, based on share-fraction/indifference-curve relationships [Eq. (26) and (27)].
(d) Basecase 3 (BASE3)